

FINAL REPORT

SKY TRANSPORTATION ATTACHMENT SYSTEM

**Subsystem of the
Unmanned Aerial Vehicle (UAV)
Human Transportation System**



Prepared for
Professor James Johnson
Dr. Pranav Bhounsule
The University of Texas at San Antonio
Department of Mechanical Engineering
1 UTSA Circle
San Antonio, TX 78249

Prepared by
Senior Design II - Team STRATOS
Daniel Jiwani
Chad Parker
Cristian Morales
William Hinojosa
Department of Mechanical Engineering
The University of Texas at San Antonio

December 5, 2018

TABLE OF CONTENTS

<u>Section</u>	<u>Page</u>
1.0 Introduction and Background	4
1.1 Technical Background	4
1.2 Review of the Effects of Damping	4
1.3 Electromagnetic Damping	5
1.4 Kinematic Diagrams of Drone and Hinged Payload	5
1.5 Statement of the Problem	5
2.0 Purpose	5
3.0 Objectives, Approach, Expected Accomplishments, and Benefits	6
3.1 Objectives	6
3.2 Approach	6
3.3 Expected Accomplishments	6
3.4 Benefits	7
4.0 Specifications	7
5.0 Concept Design	9
5.1 Initial Concept Designs	9
5.2 Selection Criteria	10
6.0 Prototype Design	11
6.1 Analytical/Experimental Methods Used for Performance and Sizing	11
6.2 Design Refinements/Optimization	11
6.3 Failure Modes and Effects Analysis	12
6.4 Material Selection and Justification	12
6.5 Diagrams Showing Physical Principles	13
6.6 Key Drawings Showing Top-Level Features and Assembly	14
7.0 Prototype Fabrication	14
7.1 Fabrication Methods	14
7.2 Assembly & Drawings	15
7.3 Bill of Materials	16
8.0 Prototype Tests	17
8.1 Test Conditions	17
8.2 Test Plan Summary	17
8.2 Test Setup and Apparatus	18
8.3 Test Results	20
9.0 Program Management	23
9.1 Personnel	23
9.2 Overall Schedule	23

9.2.1	Percent Complete	24
9.2.2	Overall Percent Complete	24
9.2.3	Personnel Assignments for Each Week	25
9.3	Financial Performance	25
9.3.1	Overall Planned Cost vs. Time Compared to Actual Cost vs. Time	26
9.3.2	Planned Material/Labor Cost by Task vs. Actual Material/Labor Cost by Task	26
10.0	Conclusions	27

LIST OF FIGURES

<u>Figure</u>		<u>Page</u>
1. 1	Drone, Payload Interaction	5
5.1	Mark 1	10
5.2	Mark 2	10
5.3	Mark 3	10
5.4	Early Concept Design	10
5.5	Final Product Illustration and Exploded View	11
6.1	Magnetic Force Diagram	13
7.1	Pin Connector (Pre-Completion)	14
7.2	Pin Connector (Final)	14
7.3	Machining for Electromagnetic Dampers (1)	15
7.4	Machining for Electromagnetic Dampers (2)	15
7.5	Pin Connection Drawing	16
8.1	Potentiometer	18
8.2	Gears to Record Oscillation	18
8.3	B&K Precision (Model 9115) Power Supply	19
8.4	Block Diagram and Waveform Chart	20
8.5	Damped Oscillation (with a 100 lb passenger mass at 15 degrees)	21
8.6	Undamped Oscillation (with a 100 lb passenger mass at 15 degrees)	21
9.1	Gantt Chart	23
9.2	Planned Cost	26
9.3	Actual Cost	26
9.4	Planned Cost vs. Actual Cost of Materials and Labor	26

LIST OF TABLES

<u>Table</u>		<u>Page</u>
4.1	Specifications	7
7.1	Cost of Parts and Labor	16
8.1	Populated Test Table	22

9.1	Percent Complete by Task	24
9.2	Week-by-Week Schedule	25
9.3	Earned Value Table	25

ACRONYMS

AWG	American Wire Gauge
GSR	Graduate Studies and Research
MH	McKinney Humanities
NI	National Instruments
STAS	Sky Transportation Attachment System
UAV	Unmanned Aerial Vehicle
UTSA	University of Texas at San Antonio

NOMENCLATURE

B	Magnetic Field
F	Force
<i>i</i>	Current
L	Length of Coil
lbs	Pounds
m	Mass
n	Number of turns of wire
r	Distance between the two objects
r_t	Distance from the point of rotation
T	Period
v	Tangential Velocity
δ	Logarithmic Decrement
ζ	Effective Damping
μ	Permeability constant

1.0 Introduction and Background

The objective of this program is to demonstrate the capabilities of an electromagnetic damping system to be able to reduce oscillation. A damping system will be required in order to provide increased stability and energy efficiency for the drone during flight, as well as increasing passenger comfort and safety. The need for damping emerges as we look into the interactions between a simply pin connected system, and the drone as it undergoes a transportation flight path. This type of flight path will require intermittent movement patterns as the drone goes to land or deliver a person. This pattern of movement described as a stop and go flight path creates oscillations for the transportation system.

1.1 Technical Background

The objective of our system is to dampen the movement in these oscillations, stopping any potential increases from a frequent stop and go flight path. This is shown in Figure 1.1. These induced oscillations create an increase in velocity relative to the drone's own speed. This increase in velocity corresponds to an increase in centripetal force as described by the equation below:

$$F = \frac{mv^2}{r_t}$$

If the drone were to counteract these oscillations on its own it would have to alter its flight path, increasing the complexity of the flight program, and possibly reducing landing precision and capabilities.

1.2 Review of the Effects of Damping

Damping plays a vital role in regulating the motion of an object. It is an effect, which tends to decrease the velocity of a moving object. There are numerous techniques that are used which include various moving, oscillating and rotating systems. These techniques include conventional friction damping, air friction damping, fluid friction damping, and electromagnetic damping.

1.3 Electromagnetic Damping

Electromagnetic damping is one of the most captivating damping techniques, which uses electromagnetically induced currents to slow down the motion of a moving object without any physical contact with the moving object. Electromagnetic induction is a marvel, in which an electromotive force is induced in a conductor when it undergoes a change in the magnetic field.

1.4 Kinematic Diagrams of Drone and Hinged Payload

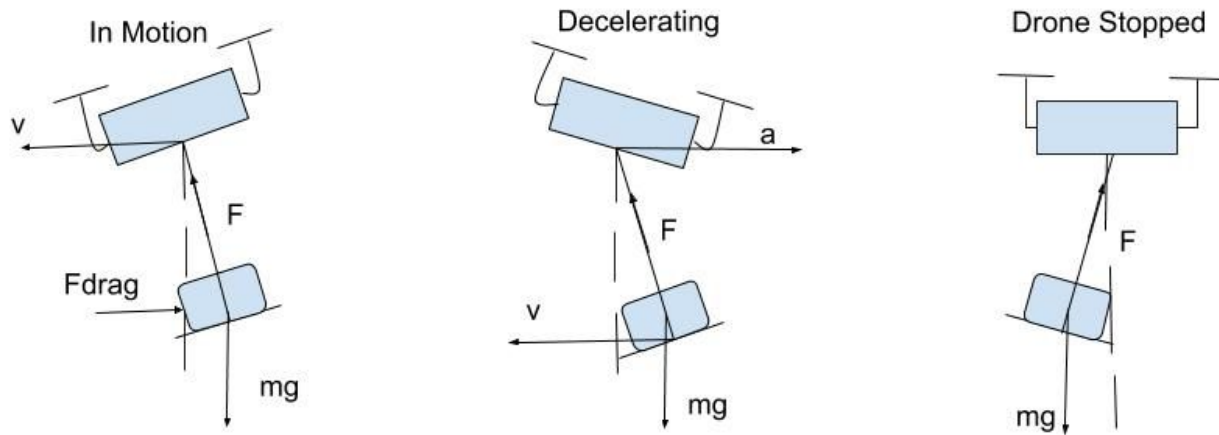


Figure 1.1: Drone, Payload Interaction

1.5 Statement of the Problem

Ultimately using a pin connected system allows for more variability in passenger and cargo loads, but comes with the additional problem of oscillations that will occur as the drone navigates around its environment. The busier the environment the more complex the flight path and greater likelihood of increasing start and stop flight patterns. Oscillations are guaranteed in this type of interaction and it is imperative to dampen these motions to allow for a more controlled and efficient flight.

2.0 Purpose

UTSA engineering, in association with Dr. Pranav Bhounsule, is developing a heavy payload drone for automated aerial transportation as an effort to bypass traffic. The system puts the drone over the head of the passenger, using two connecting rods to carry the passenger. This puts the

passenger in pendulum motion, which can put the drone in an unstable flight condition which wastes power, stresses the system structure, and is dangerous for the passenger. To assist their efforts Team Stratos designed an electromagnetic damping system to reduce the oscillation of the passenger weight, and a structure to test the electromagnetic dampers in a mock model of the attachment system.

3.0 Objectives, Approach, Expected Accomplishments, and Benefits

3.1 Objectives

The main objective of this project was to research damping with the use of an electromagnetic damper and a data acquisition system as it pertains to decreased settling times and centripetal force on the drone system when compared to the undamped drone. Our target reduction in oscillation is 20%, meaning the effective damping should increase by 20% when compared to the undamped model. Since this is a testing device, it should also emulate the maximum passenger and system weight, meaning the structure should also be designed to support the maximum load of 200 lbs while being at or below 200 lbs itself.

3.2 Approach

Since the payload drone for which the team is designing for is in its infancy, the team did not have a payload drone to work with in the design process. This means that the payload drone's attachment system had to be modeled rather than design a custom attachment mechanism. The modeled system was designed to have the same maximum weight as the developed system, 200 lbs, and was used to test oscillation with 3 different passenger weight and at 2 different angles, for both the undamped and damped system. The testing parameters were as follows: system weight of 190 lbs, testing weight of 100 lbs, 150 lbs, and 200 lbs, 4 electromagnets wrapped in 14 AWG enameled copper wires, and 2 testing angles at 15° and 25°.

3.3 Expected Accomplishments

With the electromagnetic dampers, the team expected the settling time to decrease from the natural settling time. As data is collected detecting the oscillation of the system, it is to be

expected that the rate at which the amplitudes of the oscillation decrease and meet will increase with the effect of the magnetic dampers (see Appendix C for test report).

3.4 Benefits

As described in the purpose, in pendulum motion, the weight of the passenger can cause unstable flight conditions which wastes power, stresses the system structure, and could cause flight failure. The kinematics of these effects were discussed in section 1 of this report. To add to this, the increase in oscillatory motion could also increase passenger anxiety in the UAV Human Transportation System. Therefore, since this system decreases oscillation it in effect reduces power used by the drone for stability, increases the structural integrity, reduces the likelihood of a system failure, and reduces passenger anxiety.

4.0 Specifications

The specifications in Table 4.1 discusses the physical specifications of our design and the functionality of how our design will operate while underneath the UAV. Table 4.1 goes into detail about material to be used, weight requirements, electrical systems, sensors, electromagnetic dampers, rods, oscillation, etc. Each of these requirements play a significant role in the overall design of the Sky Transportation Attachment System.

Table 4.1: Specifications

Spec. No.	Item	Requirement
3.2.3	Metals	Metals shall not have a density greater than 7.874 g/cm ³
3.2.4	Non-Metals	NFPA 704 Standards
3.3.1	Weight	the Total Weight of the STAS and it passenger shall not exceed 400 pounds
3.3.1.1	Passenger	Maximum weight shall not exceed 200 pounds

	Weight	
3.3.1.2	System Weight	Maximum weight shall not exceed 200 pounds
3.3.2	Electrical Systems	There shall also be consideration for the operational temperature of the battery and its surroundings so as to increase the efficiency and product live as well as to avoid the destruction of the electronics and of the STAS itself
3.3.2.1	Sensors	Sensors shall be in accordance with the IEEE STD 2700-2017 Institute of Electrical and Electronics Engineers Standard for Sensor Performance Parameter Definitions.
3.3.2.3	Battery Cables	A battery terminal non-conductive protective cover shall be provided to the battery and shall have specified indicators for cable polarity.
3.3.2.4	Battery Box	A non-metallic, vented, battery box shall be provided to retain and protect the batteries during operation, as well as to protect other vulnerable materials and systems in the STAS.
3.3.4	Oscillation	To counteract simple harmonic motion, the system will rely on the use of electromagnetic dampers
3.4.1.1	Rods	Must be made of a non-corrosive metal. The rods must sustain the maximum payload of the STAS. Magnets located at the top of the rod. The polarity of the magnet must be opposite of that of the electromagnet.
3.4.1.2	Pin Connections	The pin connections must support the maximum payload

3.4.1.3	Electromagnetic Dampers	The core of this magnet shall be cast iron. A coil of wire shall be wrapped around the iron core. The electromagnets must have an opposite polarity of the magnets positioned on the rods.
3.5	Environmental Requirements	The STAS shall be capable of being stored, maintained and operated under the following environmental conditions typical to South Central Texas.
3.6	Transportability	The STAS shall be capable of being transported by automotive, locomotive, or aeronautical transportation.

5.0 Concept Designs

The team generated some early concept design for our project, but one of our most recent concept designs consisted of the use of translational tuned mass damper. This concept consisted of using two translational tuned mass dampers that were placed perpendicular to each other in the X plane and parallel in the Y plane. These tuned mass dampers consisted of stepper motors, guided track, and weights. After researching both translational tuned mass damping systems and electromagnetic damping systems the team took careful consideration in changing from a translational tuned mass damper system to an electromagnetic damping system. Through early theoretical calculations the team determined that the electromagnetic damping system would have an overall greater reduction in oscillation.

5.1 Initial Concept Designs

During Senior Design 1, the team developed three concept design to meet the overall objective, to design a support system for UAV human transportation. Figures 5.1 through 5.3 display the three concept designs.



Figure 5.1: Mark 1

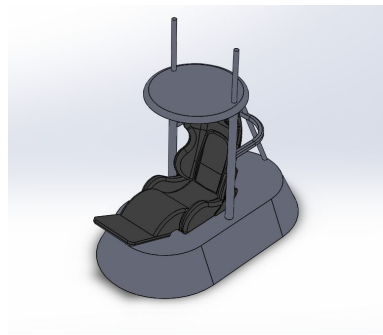


Figure 5.2: Mark 2

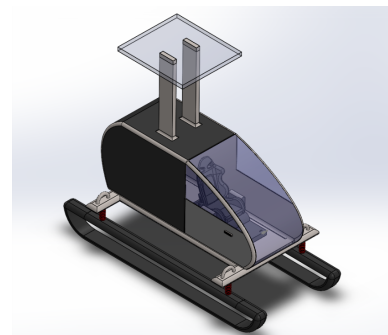


Figure 5.3: Mark 3

5.2 Selection Criteria

For the selection process of our design, the team had decided to choose Mark 2 and build around that design. The final design of the system is shown below in Figure 5.4.

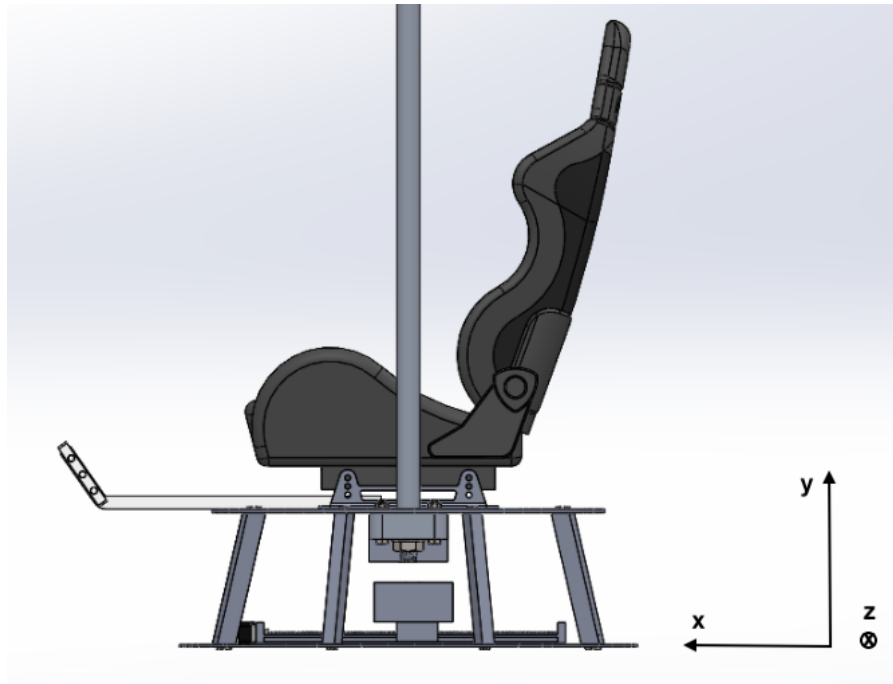


Figure 5.4: Early Concept Design

However, at the beginning of Senior Design 2 semester, the team and our sponsor had decided to not focus on building a final design for UAV human transportation. Instead, we should consider creating a model for our project and focus on a single principal, reducing oscillation while the system is in motion. Therefore, the team scrapped the final design that was selected in Senior

Design 1 and created a model that would implement the electromagnetic dampers. Figure 5.5 shows the final design that was selected and then used for fabrication and testing.

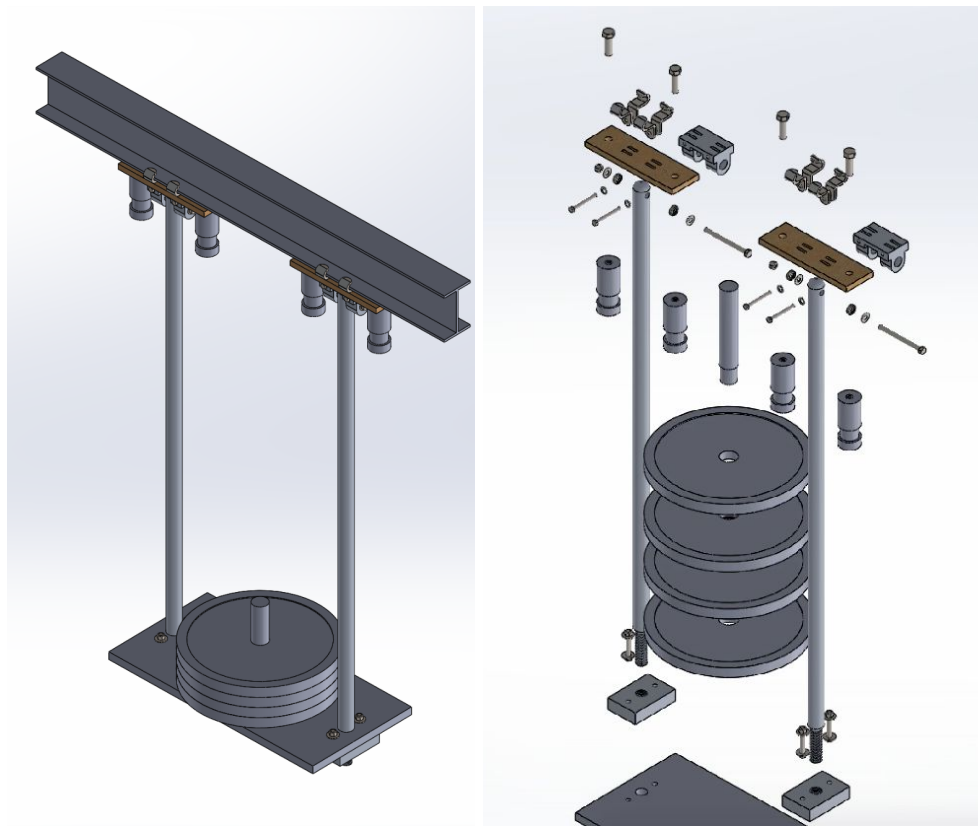


Figure 5.5: Final Product Illustration and Exploded View

6.0 Prototype Design

6.1 Analytical/Experimental Methods Used for Performance and Sizing

In order to accurately test damping of oscillations at different weight intervals the system needed to hold and maintain the different sets of weight in a controlled manner. If a prototype was made to hold a person comfortably then control of the weights would be questionable. As you can see from the model there exists a weight bar and rigid base to hold the 200 lbs required to simulate a human passengers weight. The model was also designed in a way to accurately portray the weight seen in the teams previous carriage concept.

6.2 Design Refinements/Optimization

In order to reduce effects of friction, two sets of high load radial bearings were placed in each pin connector. This allowed for smooth even oscillations, and an undamped motion that lasted

longer than the myDAQ system was able to handle. There existed rigid connections with no wobbling between the system, and the I-beam for the angles tested.

6.3 Failure Modes and Effects Analysis

The main criteria of failure for this project, aside from system failure, would be through testing of the device. If at any point, or if there was any concern of the I-beam being deformed from the test which would result in the immediate cancellation of the project by UTSA facilities. Initial steps for this process were to conduct a simulation to determine if plastic deformation will occur. Once weight limits were set testing could be conducted. Intended use will result in no failure to the parts themselves.

The tests conducted can be condensed to these basic steps:

- 1) Hoist system to desired angle
- 2) Start myDAQ system
- 3) Release system
- 4) Collect data

Main sources of error in testing can occur during each step in the process. Reaching and maintaining the intended testing angle, retaining the intended testing angle, and release the device quickly without causing unwanted damping. These failures can be controlled with the use of an outside observer positioned to see the angle of release with the help of a marking system.

6.4 Material Selection and Justification

For our material selection, the team chose materials that would be best suitable for the design of our system. First, the selection of Aluminum 6061-T6 was chosen because of its ability to be high in strength, light weight, and good workability while machining. Aluminum 6061-T6 was used for our mounting brackets, pin connectors, and the weight pin. Second, the selection of Steel was chosen for its high tensile strength and low cost. Steel was used for our base plate and the I-beam clamps; the base plate supported the weights we used during the testing phase. Third, the selection of Cast Iron was chosen because of it has decent permeability and the cost of the material was within our budget. Cast Iron was used for the electromagnetic dampers in our

design. Lastly, the selection of Wood because its low cost and easy workability. Wood was used for our mounting bracket spacers that were placed in-between the pin connectors and the I-beam with the clamps inserted through them.

6.5 Diagrams Showing Physical Principles

Calculating the force of the magnets that are imparted into the system requires knowledge of the magnetic fields produced by the magnets and the rod. The equation used for the magnets is shown below:

$$B = \frac{\mu n i}{L}$$

Where B is the magnetic field measured in Teslas, μ is the permeability constant, n is the number of turns, i is the current measured in Amperes, and L is the length of the coil. With this calculated value and the value for the rods magnetic field found online, force can be calculated from the equation below:

$$F = \frac{\mu_0 B_1 B_2}{4\pi r^2}$$

Where μ_0 is the permeability of free space, B_1 is the magnetic field of the electromagnets, B_2 is taken as the magnetic field of a bar magnet, and r is the distance between the two objects. From these equations it is possible to see the force imparted into the system.

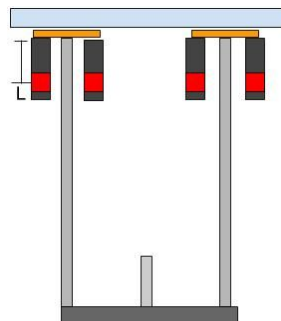


Figure 6.1: Magnetic Force Diagram

From this viewpoint it is shown that the magnets interact with the top portion of the system whose main magnetic field interaction occurs length L from the top.

6.6 Key Drawings Showing Top-Level Features and Assembly

In appendix D isometric views, and exploded views of the system can be shown, along with the brackets and fasteners needed to attach the system to the I-beam. The only parts not shown are the copper wiring and power supply unit.

7.0 Prototype Fabrication

7.1 Fabrication Methods

Fabrication of this project began during the month of October 2018. The team purchased raw materials from the Westbrook Metals and Vestel Steel. The large parts (such as the steel plate and connection rods) were sent to ITM incorporated. The smaller parts (such as the pin connectors, mounting brackets, electromagnets, and weight pin) were taken to the UTSA machine shop. Fabrication was completed on November 8, 2018

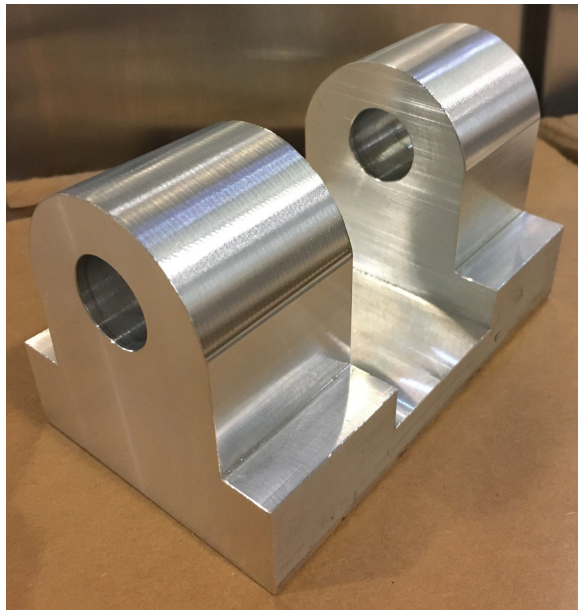


Figure 7.1: Pin Connector (Pre-Completion)



Figure 7.2: Pin Connector (Final)



Figure 7.3: Machining for Electromagnetic Dampers (1)

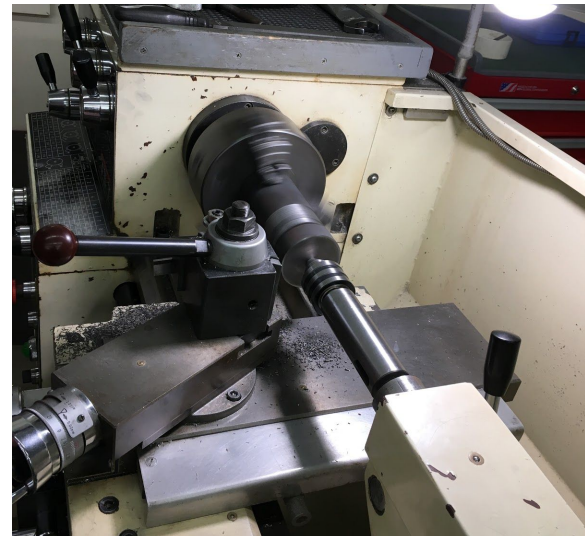


Figure 7.4: Machining for Electromagnetic Dampers (2)

7.2 Assembly & Drawings

The apparatus was then assembled, first securing the pin joints and mounting bracket to the I-beam, then connecting the data acquisition system and the electromagnets to the mounting bracket, and finally attaching the plate to the connection rods.

The final assembly consists of the following parts:

Pin Connector (2)	Beam Clamps (8)	Weight Pin (1)
Steel Plate (1)	Electromagnets (4)	Weights (7)
Connection Rod (2)	Mounting Bracket (2)	Wood (2)

For the assembly of the STAS onto the I-beam (for testing), the first step would be to attach the clamps. The clamps will then be slipped through a wooden mounting bracket and into the slots of the pin connector. These clamps will then be secured using bolts. Next, the connection rods must be placed between each pin connector, after the bearing has been placed in the pin connector hole. Once the connection rods have been assembled, the steel plate is placed through the threads of the connection rods and then secured at the bottom with a mounting bracket. Figure 7.5 displays a critical part for the purpose of testing - the pin connector.

For the image of the final assembly and the rest of the drawings, please refer to Appendix D.

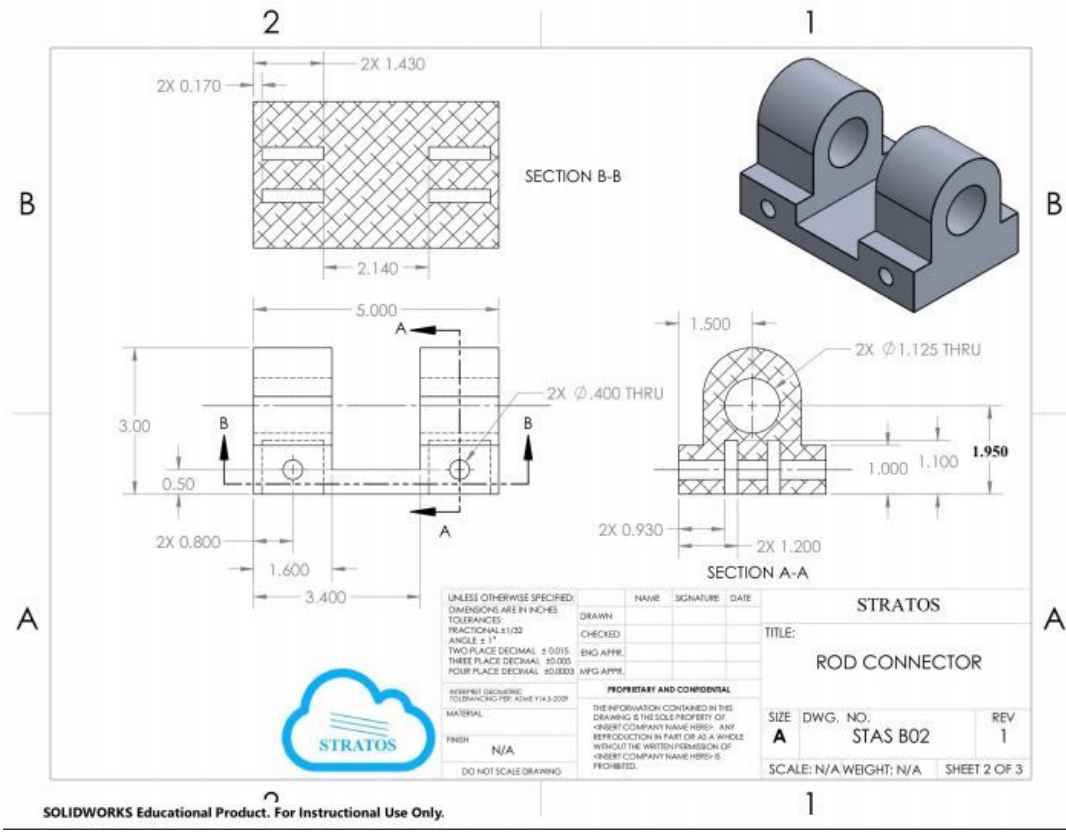


Figure 7.5: Pin Connection Drawing

7.3 Bill of Materials

Table 7.1: Cost of Parts and Labor

Parts and Labor	Quantity	Unit Price	Cost
Connection Rods	2	\$77.00	\$154.00
Weight Pin	1	\$23.00	\$23.00
Mounting Bracket	2	\$25.00	\$50.00
Pin Connector	2	\$26.00	\$52.00
Steel Plate	1	\$260.00	\$260.00
Connection Rods (Labor)	2	\$175.00	\$350.00
Steel Plate (Labor)	1	\$395.00	\$395.00
Copper Wires	1	\$77.35	\$77.35
Clamps	4	\$15.05	\$60.20

Cast Iron (Electromagnets)	2	\$40.82	\$81.64
	Total		\$1,503.19

8.0 Prototype Tests

8.1 Test Conditions

For the testing phase of this project, the team began scouting a suitable location to suspend our load and test oscillation. When searching for a test facility, there were a few criteria that the team had to keep in mind. The first, the room must have an I-beam stable enough to hold a 400-pound mass. This I-beam must have at least six feet of clearance from the beam to the ground. The location of where this I-beam is located is preferred to be indoors. If this beam was located outdoors, then due to weather conditions in San Antonio in the month of October and November, our data would be introduced to another form of error. Next, the test site must also be accessible to an electrical outlet. Finally, the test site must be secluded from the public. The test site found is located on the ground floor of the McKinney Humanities (MH) building. The site is restricted to all students and staff member, however, representatives from Graduate Studies and Research (GSR) have allowed us to set up our assembly and conduct our tests from November 1st to November 12th.

For data acquisition, the team used a myDAQ to read the voltage of a potentiometer that was positioned at the top (next to the pin connector). The team constructed a block diagram of LabView in order to get a graph of oscillation from the potentiometer. On the team received a graph of the undamped and damped oscillation, the effective damping was calculated using the logarithmic decrement.

8.2 Test Plan Summary

Preparation of the testing site commenced with the suspension of the STAS to the I-beam in the test site. The potentiometer was then wired and fastened to the wooden mounting bracket and connected to the NI myDAQ. The system was then inspected by the engineers before the tests begin. Testing procedure consists of an engineer running the data acquisition system and signaling the team to hoist the system at the first testing angle and the first testing weight. The

data acquisition engineer then signaled the team to release the system and data was recorded by the NI myDAQ. Once the NI myDAQ collected 3 minutes of data, the system was then halted, and the data exported. The same angle and weight were then tested 2 more times, before moving to the dataset. Finally, once all the datasets were collected for the undamped system, the magnetic dampers were activated and the same tests were run for the damped system.

8.2 Test Setup and Apparatus

First, the team inspected the STAS' various parts for quality assurance, ensuring that all parts were within dimensional tolerance and were made of the correct materials. When all parts pass inspections, the team then attached the STAS to the steel I-beam, following the Operations Manual setup instructions. Safety tests were then ran to ensure that the I-beam and the STAS can safely handle maximally loaded motion at the different angles. During this process, we discovered that the I-beam that the STAS was clamped to would rotate at higher angles and the clamps would shake with the oscillation. For safety and to avoid causing structural damage, we eliminated 30° and 45° from our test matrix. The first piece of equipment necessary to record oscillation is the potentiometer. The potentiometer is located at the top of the structure, next to the pin connector. There are two gears that are attached to the bolt (that is rotating along with the structure) and the potentiometer, as shown in Figures 8.1 and 8.2 below.



Figure 8.1: Potentiometer

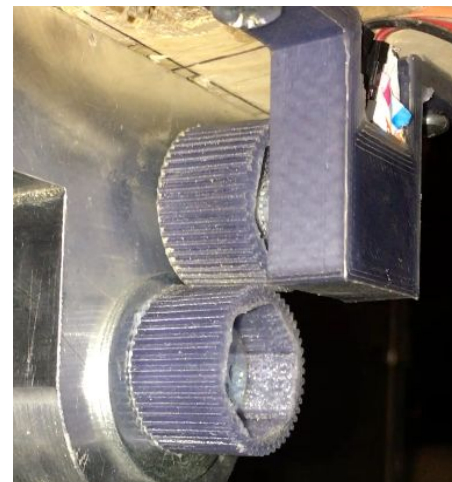


Figure 8.2: Gears to Record Oscillation

The next piece of equipment that is necessary for this experiment is the bearings. There are four bearings that are pressure-fitted into the pin connectors. These bearings will reduce friction as the structure is oscillating and allow the team to effectively record data.

The final two pieces of equipment have been used to supply power to the electromagnets. The first is the 14 gauge enameled copper wire that is wrapped around the cast iron core of the electromagnets. With these wires, the team can supply no more than 15 amps of current. Next, the B&K Precision power supply, that was loaned to us from our sponsor, was used to supply power to the electromagnets.



Figure 8.3: B&K Precision (Model 9115) Power Supply

To record data, a potentiometer is used to record oscillation. To read the incoming voltage of the potentiometer, the team used a myDAQ from National Instruments. First, the team constructed a block diagram with the NI myDAQ and potentiometer, as shown in Figure 8.4 below. The team is then able to create a waveform chart, which allows the user to read the voltage of the potentiometer.

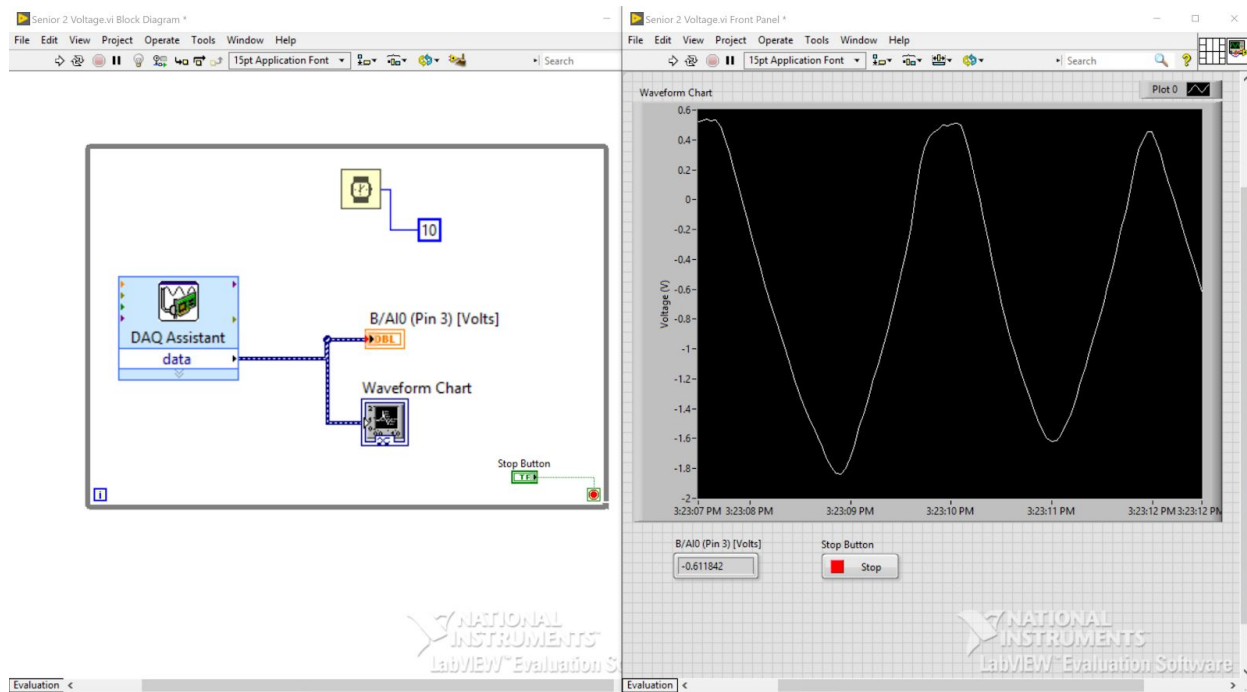


Figure 8.4: Block Diagram and Waveform Chart

8.3 Test Results

In this experiment, the team graphed the oscillation for three passenger masses at two different angles of attack. For each test performed, there were at least three trials conducted. Therefore, the total number of tests performed was 36.

Figures 6.1 and 6.2 show the oscillation graph of the damped and undamped system, respectively, with a 100-pound passenger mass at an angle of 15 degrees from the vertical axis. The two graphs are plotted with the voltage with respect to time.

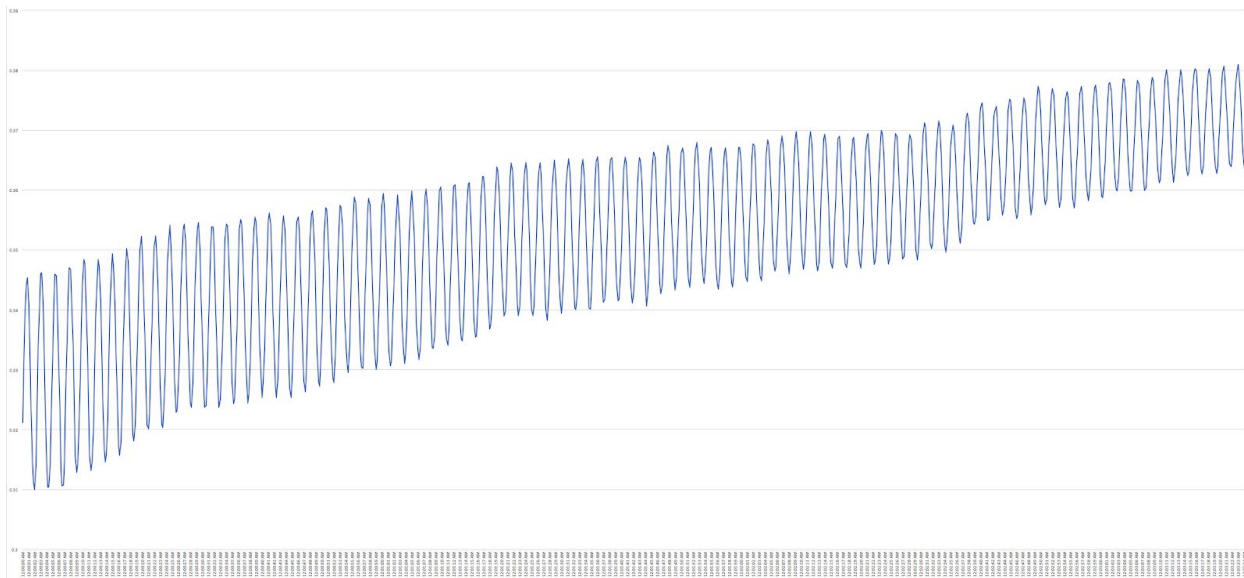


Figure 8.5: Damped Oscillation (with a 100 lb passenger mass at 15 degrees)

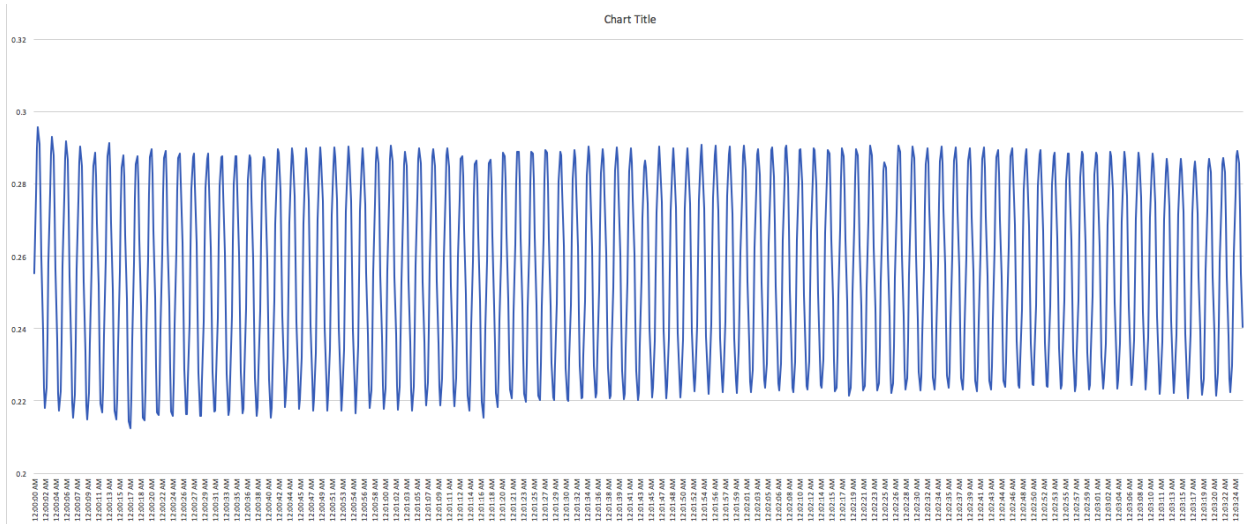


Figure 8.6: Undamped Oscillation (with a 100 lb passenger mass at 15 degrees)

Once the team received a graph of oscillation, a few points, at random, were chosen to find the effective damping. During the damped trials, the graph was not plotted on the same level, similar to the undamped graph. Instead, the graph began to shift up, as shown in Figure 8.1. To find the effective damping of these trials, the team first calculated the difference between the upper and lower limit of the graph for multiple points in time. With this, the effective damping for the

damped trials was calculated. The effective damping (ζ) is solved for with the following equation

$$\zeta = \frac{\delta}{\sqrt{4\pi^2 + \delta^2}}$$

where the logarithmic decrement (δ) is given by the following equation

$$\delta = \ln \left[\frac{x(t)}{x(t+T)} \right]$$

Table 8.1 below displays the period (T) and effective damping calculated for each case (undamped and damped) at the two angles it was released from.

Table 8.1: Populated Test Table

Test Number	Angle from vertical axis	Passenger Mass (lb)	T (s)	ζ
1	15° Undamped	100	3	0.00095966
2		150	2	0.00046318
3		200	3	0.00014795
4	25° Undamped	100	2	0.00144224
5		150	2	0.00043945
6		200	3	0.00029883
7	15° Damped	100	2	0.10663223
8		150	3	0.06055912
9		200	2	0.05369636
10	25° Damped	100	3	0.10068529
11		150	3	0.0759203
12		200	3	0.06475203

As shown by the populated table and Figures 8.5 and 8.6 (which displays the undamped and damped graph, respectively), the effective damping with the use of electromagnetic dampers is greater than the effective damping without it. Table 8.1 displays the effective damping of the system with and without the use of the electromagnetic dampers. From the table, the effective damping with a passenger mass of 100 pounds (regardless of whether or not the electromagnets

are in use) is greater than the effective damping with a 150 and 200-pound passenger mass. As predicted, the electromagnetic dampers have been able to effectively increase damping.

9.0 Program Management

9.1 Personnel

For this project, the team would like to acknowledge Dr. Pranav Bhounsule for sponsoring this project and for his continuous support as our mentor. Next, Professor James Johnson for pushing our limits and helping the team get back on track. Finally, the UTSA staff at Graduate Research and Studies and facilities in assisting with the test site acquisition.

9.2 Overall Schedule

Figure 9.1 below displays the Gantt Chart which shows the all of the major assignments completed by the team in the Senior Design 2 semester.

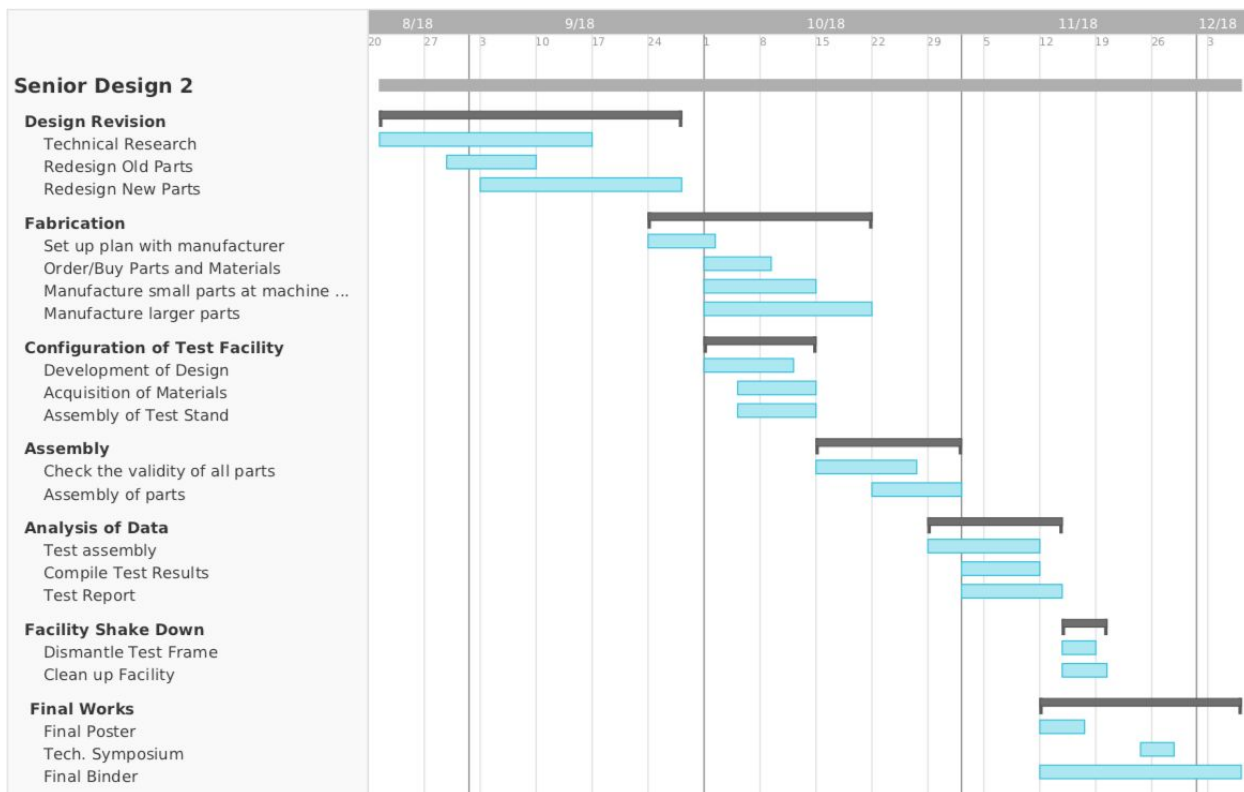


Figure 9.1: Gantt Chart

9.2.1 Percent Complete

Table 9.1 shows a detailed layout of the Gantt Chart which lists all of the major tasks completed with the date at which this task began and ended.

Table 9.1: Percent Complete by Task

Task		Start Date	End Date	Percent Completion
Design Revisions	Technical Research	Aug-21	Sep 14	100%
	Redesign Old Parts	Aug-29	Sep 7	100%
	Redesign New Parts	Sep-3	Sep 26	100%
Fabrication	Set up plan with manufacturer	Sep 24	Oct 1	100%
	Order Parts and Materials	Oct 1	Oct 12	100%
	Fabrication at ITM	Oct 1	Oct 19	100%
	Fabrication at UTSA machine shop	Oct 8	Nov 5	100%
Assembly	Check parts with their drawing	Oct 24	Nov 2	100%
	Assembly of Parts	Oct 31	Nov 6	100%
Configuration of Test Facility	Development of Design	Oct 25	Oct 26	100%
	Acquisition of Materials	Oct 29	Oct 31	100%
Testing and Analysis of Data	Test Assembly	Nov 1	Nov 9	100%
	Testing	Nov 7	Nov 12	100%
	Compile Test Results	Nov 7	Nov 12	100%
	Test Report	Nov 8	Nov 13	100%
Facility Shakedown	Dismantle Test Assembly	Nov 14	Nov 16	100%
	Clean up Facility	Nov 16	Nov 16	100%
Final Work	Final Poster	Nov 12	Nov 15	100%
	Tech. Symposium	Nov 27	Nov 27	100%
	Final Report	Nov 14	Dec 5	100%
	Final Binder	Nov 12	Dec 5	100%

9.2.2 Overall Percent Complete

The following section lists the percent complete during Senior Design up to date.

Senior Design 1 (January 8, 2018 - May 17, 2018): 100%

Senior Design 2 (August 20, 2018 - December 5, 2018): 89%

9.2.3 Personnel Assignments for Each Week

The following table lists the major tasks that were completed for each week and the hours each team member has spent.

Table 9.2: Week-by-Week Schedule

Week	Start Date	End Date	Major Weekly Task(s)	Team Members				Total Hours
				Chad Parker	Cristian Morales	Daniel Jiwani	William Hinojosa	
1	Aug-20	Aug-26	Class, Presentation	5	4.5	6	5	20.5
2	Aug-27	Sep-2	Revise Drawings, Research, Meeting	21.5	18.5	23	18	81
3	Sep-3	Sep-9	Redesign, Revision of Specifications	23	25.5	25	23	96.5
4	Sep-10	Sep-16	Class, Meeting, Redesign, Test Plan	19.75	22	24	20	85.75
5	Sep-17	Sep-23	Redesign, Research, Operations Manual	13	14	14.75	14.75	56.5
6	Sep-24	Sep-30	Drawings, Presentation, Research, Test Plan	13	13	15.5	16	57.5
7	Oct-1	Oct-7	Meeting, Presentation, Ordering Parts	13	13	17.75	11	54.75
8	Oct-8	Oct-14	Presentation, Ordering Parts, Program Controller	10	15	10.5	8	43.5
9	Oct-15	Oct-21	Meeting, Fabrication, Ordering Parts	8	6	7.25	2.75	24
10	Oct-22	Oct-28	Test Site, Fabrication, Abstract, Thematic Outline	5	10	7	6.75	28.75
11	Oct-29	Nov-4	Test Site, Fabrication, Poster, Meetings, Assembly Setup	5	12	12.5	8.5	38
12	Nov-5	Nov-11	Test Setup, Testing, Test Report	29	41	44.25	36	150.25
13	Nov-12	Nov-18	Testing, Test Report, Clean up test site	19	13	25.5	20	77.5
14	Nov-19	Nov-25	Tech Symposium, Final Presentation	8	13	13	8	42
15	Nov-26	Dec-2	Final Binder	14	14	27	11	66
Total				206.25	234.5	273	208.75	922.5

9.3 Financial Performance

The following table discusses the projects earned value from the team members contribution.

Table 9.3: Earned Value Table

Task	Start Date	End Date	Budget	BCWS	BCWP	ACWP	SPI	CPI	CSI
Senior Design 1	Jan-9	May-12	\$100,000	\$100,000	\$100,000	\$105,000	1.00	0.95	0.95
Design Revision	Aug-21	Sep-30	\$10,000	\$10,000	\$10,000	\$11,000	1.00	0.91	0.91
Test Plan	Aug-21	Sep-13	\$5,000	\$5,000	\$5,000	\$4,000	1.00	1.25	1.25
Operations Manual	Sep-13	Sep-20	\$5,000	\$5,000	\$5,000	\$3,750	1.00	1.33	1.33
Acquire Materials	Sep-24	Oct-10	\$3,000	\$3,000	\$3,000	\$2,550	1.00	1.18	1.18
Fabrication	Oct-5	Oct-26	\$10,000	\$10,000	\$10,000	\$8,500	1.00	1.18	1.18
Test Facility Setup/Shakedown	Oct-29	Nov-4	\$7,500	\$7,500	\$7,500	\$5,625	1.00	1.33	1.33
Testing	Nov-5	Nov-11	\$10,000	\$10,000	\$10,000	\$9,500	1.00	1.05	1.05
Test Report	Nov-5	Nov-13	\$5,000	\$5,000	\$5,000	\$3,250	1.00	1.54	1.54
Final Presentation	Nov-13	Nov-28	\$5,000	\$5,000	\$5,000	\$3,750	1.00	1.33	1.33
Final Binder	Nov-1	Dec-5	\$10,000	\$10,000	\$10,000	\$8,500	1.00	1.18	1.18
Total			\$170,500	\$170,500	\$170,500	\$165,425	1.00	1.03	1.03

9.3.1 Overall Planned Cost vs. Time Compared to Actual Cost vs. Time

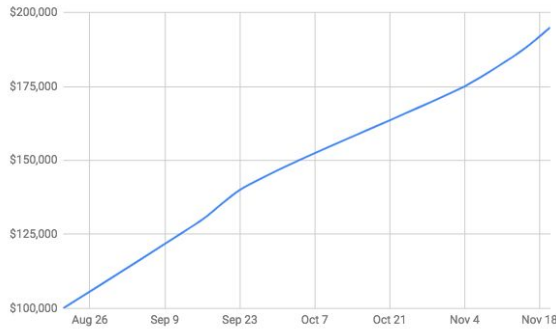


Figure 9.2: Planned Cost

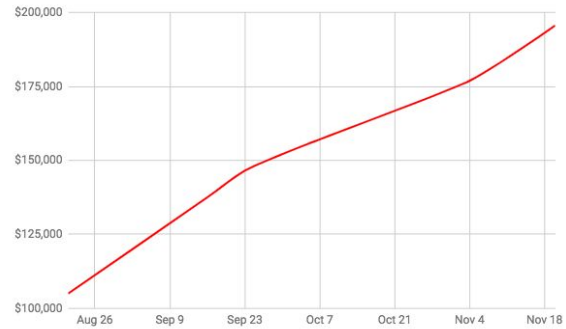


Figure 9.3: Actual Cost

9.3.2 Planned Material/Labor Cost by Task vs. Actual Material/Labor Cost by Task

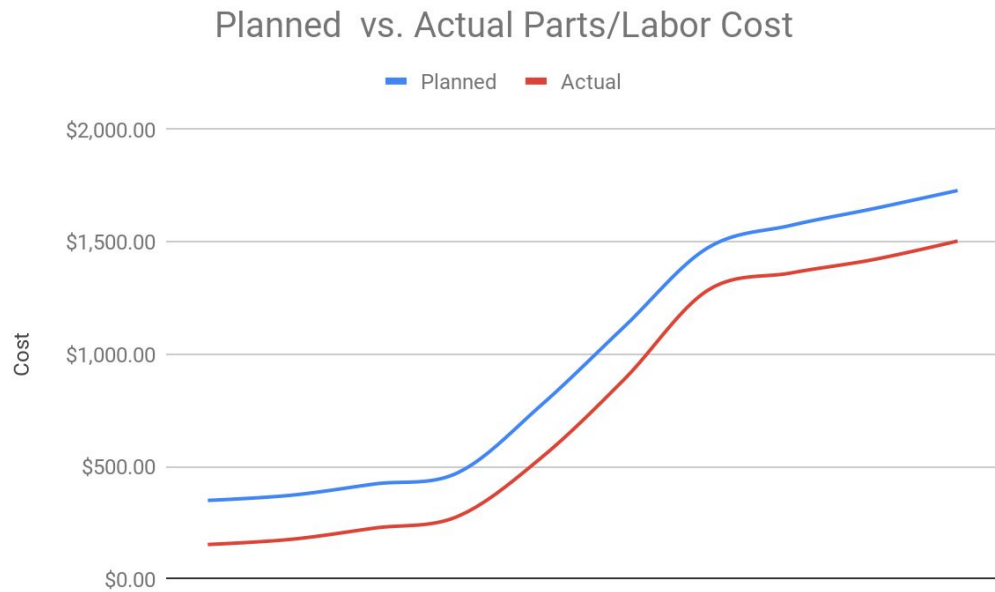


Figure 9.4: Planned Cost vs. Actual Cost of Materials and Labor

10.0 Conclusions

The purpose of this project was to find a way to reduce the oscillation that accompanies pendulum motion, so that the UAV Human Transportation Drone can have a more stable flight, the structural integrity could increase, passenger safety could increase, and passenger anxiety could decrease. To solve this the team designed,built, and tested an electromagnetic damping system and a structure to test the damping coefficients of the system at 3 weights, and 2 angles. What was found when testing the oscillation of the damped system versus the undamped system was that as predicted, the electromagnetic dampers reduced the settling time of the oscillation, and effectively increase the effective damping of the system. While the goal of the project was a success, the team suggests that a major increase in the current supplied, and power of magnets is needed to reach the goal of a truly effective method of damping the system. This is because the settling time for the damped system was still greater than 3 minutes, and would mean the drone would have to wait over 3 minutes for the system to stabilize if operated as currently designed. Furthermore, the connecting rods could be redesigned to have a stronger opposing magnetic force to the electromagnets to increase the damping by magnetic attraction. Other mechanical methods could also be used to increase the effective damping of the system, such as an aerodynamic damper, which increases damping by having an higher drag coefficient. Despite these suggestions, this design achieved its intended purpose, and can be used as an acceptable method of reducing oscillation.

TEST REPORT

SKY TRANSPORTATION ATTACHMENT SYSTEM



Prepared for
Professor James Johnson
Dr. Pranav Bhounsule
The University of Texas at San Antonio
Department of Mechanical Engineering
1 UTSA Circle
San Antonio, TX 78249

Prepared by
Senior Design II - Team STRATOS
Daniel Jiwani
Chad Parker
Cristian Morales
William Hinojosa
Department of Mechanical Engineering
The University of Texas at San Antonio

December 5, 2018

TABLE OF CONTENTS

<u>Section</u>	<u>Page</u>
1.0 Introduction	6
1.1 Description, Purpose of Testing, and Scope	6
1.2 Features to be Tested	7
2.0 Test Evaluation Criteria	7
2.1 Compliance Matrix	7
2.2 Pretest Uncertainty Analysis	8
2.3 Performance Test Matrix	9
2.4 Types of Test Considered	9
3.0 Test Facility	10
3.1 Location	10
3.2 Structural Integrity of the Beam	11
3.3 Instrumentation and Equipment	12
3.4 Data Systems used for Testing	13
4.0 Test Description	13
4.1 Test Conditions	14
4.2 List of Instruments Required	14
4.3 Calibration Procedures and Traceability	14
5.0 Data Reduction and Analysis	14
5.1 Analysis Methods	14
5.2 Verification of Test Results	17
5.3 Error Analysis	18
6.0 Reported Results	18
6.1 Populated Table	20
6.2 Results Support of Conclusion	20
7.0 Schedule	20
8.0 Conclusions and Recommendations	22
9.0 Communication	23
A.1 Beam Deflection Calculations	24
A.2 Design Specifications	25

LIST OF FIGURES

<u>Figure</u>	<u>Page</u>
1.1 Drone and Payload	6
2.1 Poles of an Electromagnet	10
3.1 Testing Room	11
3.2 Testing Room	11
3.3 Potentiometer	12
3.4 Gears to record oscillation	12
3.5 B&K Precision (Model 9115) Power Supply	12
3.6 Block Diagram and Waveform Chart	13
5.1 Analysis of Undamped Trials (15°, 100 lbs)	15
5.2 Analysis of Damped Trials (15°, 100 lbs)	15
5.3 Analysis of Undamped Trials (25°, 100 lbs)	15
5.4 Analysis of Damped Trials (25°, 100 lbs)	15
5.5 Analysis of Undamped Trials (15°, 150 lbs)	16
5.6 Analysis of Damped Trials (15°, 150 lbs)	16
5.7 Analysis of Undamped Trials (25°, 150 lbs)	16
5.8 Analysis of Damped Trials (25°, 150 lbs)	16
5.9 Analysis of Undamped Trials (15°, 200 lbs)	17
5.10 Analysis of Damped Trials (15°, 200 lbs)	17
5.11 Analysis of Undamped Trials (25°, 200 lbs)	17
5.12 Analysis of Damped Trials (25°, 200 lbs)	17
5.13 Oscillation Graph with a 200 lb passenger mass at 15 degrees	18
6.1 Damped Oscillation (with a 100 lb passenger mass at 15 degrees)	19
6.2 Undamped Oscillation (with a 100 lb passenger mass at 15 degrees)	19
7.1 Gantt Chart	21

LIST OF TABLES

<u>Table</u>	<u>Page</u>
2.1 Compliance Matrix	7
2.2 Performance Test Matrix	9
6.1 Populated Test Table	20
7.1 Percent Complete by Task	22

ACRONYMS

GSR	Graduate Research and Studies
MH	McKinney Humanities
NI	National Instruments
STAS	Sky Transportation Attachment System
UTSA	University of Texas at San Antonio

NOMENCLATURE

T	Period
t_i	Settling Time for undamped system
t_d	Settling Time for Damped System
ζ	Effective Damping

A Test Plan for the Sky Transportation Attachment System

1.0 Introduction

The purpose of this project is to aid in the development of drone assisted individual travel. The goal is to be able to create an attachment system that can be used for drones suitable to carry up to 400 pounds. In order to reduce weight and inertia, a simple pin connected system will be used. This, however, brings in the problem of oscillations that occur during the drones flight plan.

The objective of our system is to dampen the movement in these oscillations, stopping any potential increases from a frequent stop and go flight path. This is shown in the figure below:

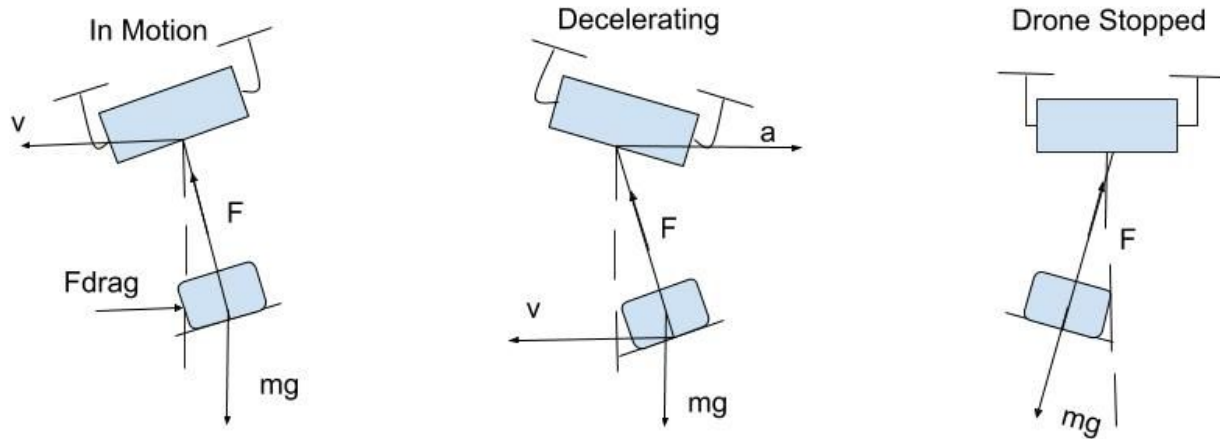


Figure 1.1: Drone and Payload

Displacements from this interaction will interfere with the drones control system, requiring additional programming or action from the flight controller. This sort of flight path is common for when the drone is planning its landing.

1.1 Description, Purpose of Testing, and Scope

This system is made to test the effectiveness of electromagnetic dampers in aiding stability for a load carried by drone. This system simulates a point mass simply pinned connected undergoing oscillations about one axis. These tests will determine the viability of this system, compared to an undamped system. Multiple tests will be conducted at the angles shown in Table 2.2 while also having multiple weighted loads for each of these angles.

The model itself is weighted to be identical to the passenger enabled structure to provide a baseline of weight. Which was measured from a previous design that included an impact reducing safety structure. Weight will then be added to simulate passenger loads with a maximum capacity of 200 pounds.

1.2 Features to be Tested

Testing will be conducted to ensure the effectiveness of the electromagnetic dampers for the use of reducing oscillations in a simply connected, hanging payload. The electromagnets will slow down the oscillations, and the tests will show the magnitude of damping that the electromagnets will impart on the system.

2.0 Test Evaluation Criteria

Testing will require an accurate measurement of angles that can be viewed while hoisting the system into position. A steady and even release is then required to record accurate. Gears attaching the pin connector and radial potentiometer will be used to provide an accurate description of the systems changing angular displacement using the change in voltage.

2.1 Compliance Matrix

The compliance matrix, shown in Table 2.1, cross-references what relation our tests and setup have to the design specifications.

Table 2.1 Compliance Matrix

Spec. No.	Item	Requirement	Compliant
3.2.3	Metals	Metals shall not have a density greater than 0.284 lb/in ³	Yes
3.2.4	Non-Metals	NFPA 704 Standards	Yes
3.3.1	Weight	the Total Weight of the STAS and it passenger shall not exceed 400 pounds	Yes
3.3.1.1	Passenger Weight	Maximum weight shall not exceed 200 pounds	Yes
3.3.1.2	System Weight	Maximum weight shall not exceed 200 pounds	Yes
3.3.2	Electrical Systems	There shall also be consideration for the operational temperature of the battery and its surroundings so as to increase the efficiency and product live as well as to avoid the destruction of the electronics and of the STAS itself	Yes

3.3.2.1	Sensors	Sensors shall be in accordance with the IEEE STD 2700-2017 Institute of Electrical and Electronics Engineers Standard for Sensor Performance Parameter Definitions.	Yes
3.3.2.3	Battery Cables	A battery terminal non-conductive protective cover shall be provided to the battery and shall have specified indicators for cable polarity.	Yes
3.3.2.4	Battery Box	A non-metallic, vented, battery box shall be provided to retain and protect the batteries during operation, as well as to protect other vulnerable materials and systems in the STAS.	Yes
3.3.4	Oscillation	To counteract simple harmonic motion, the system will rely on the use of electromagnetic dampers	Yes
3.4.1.1	Rods	Must be made of a non-corrosive metal. The rods must sustain the maximum payload of the STAS. Magnets located at the top of the rod. The polarity of the magnet must be opposite of that of the electromagnet.	Yes
3.4.1.2	Pin Connections	The pin connections must support the maximum payload	Yes
3.4.1.3	Electromagnetic Dampers	The core of this magnet shall be cast iron. A coil of wire shall be wrapped around the iron core. The electromagnets must have an opposite polarity of the magnets positioned on the rods.	Yes
3.5	Environmental Requirements	The STAS shall be capable of being stored, maintained and operated under the following environmental conditions typical to South Central Texas.	Yes
3.6	Transportability	The STAS shall be capable of being transported by automotive, locomotive, or aeronautical transportation.	Yes

2.2 Pretest Uncertainty Analysis

For this experiment there exists a few conditions that are not ideal for testing. There is a small amount of elastic deformation in the flanges of the beam, which aid in the oscillation of the system. The wires connecting the potentiometer to the NI myDAQ system are lengthened with multiple jumper cables, it was noticed that a disturbance of these cables would cause a slight and

brief difference in voltage. There also exists difficulties in hoisting the system to larger angles so repeatable tests may become slightly different or experience rapid changes in the data gathered.

2.3 Performance Test Matrix

Table 2.2: Performance Test Matrix

Test ID	Angle from the vertical axis	Passenger Mass lb	T (s)	ti (s)	td (s)	ξ (%)
1	15° Underdamped	100				
2		150				
3		200				
4	25° Underdamped	100				
5		150				
6		200				
7	15° Damped	100				
8		150				
9		200				
10	25° Damped	100				
11		150				
12		200				

2.4 Types of Tests Considered

For the following project, performance testing is the main focus of this project, the goal of which is to showcase the use of electromagnetic dampers to reduce oscillation. During testing, the STAS is elevated at multiple angles and the oscillation is recorded with and without the use of the electromagnetic dampers.

Preliminary quality assurance inspections were done to ensure that all parts were the correct materials and were within tolerance. Next, a preliminary safety test was done to ensure that the system and the I-beam would not fail at maximally loaded motion. A general test of the electromagnetic dampers must also be performed. The electromagnets are wrapped in such a manner where one end will have a south pole and the opposite end will have a north pole. Figure 2.1 displays how the electromagnet must be constructed to showcase the polarity. A general test must be conducted to verify that the poles of the electromagnet are in the correct form.

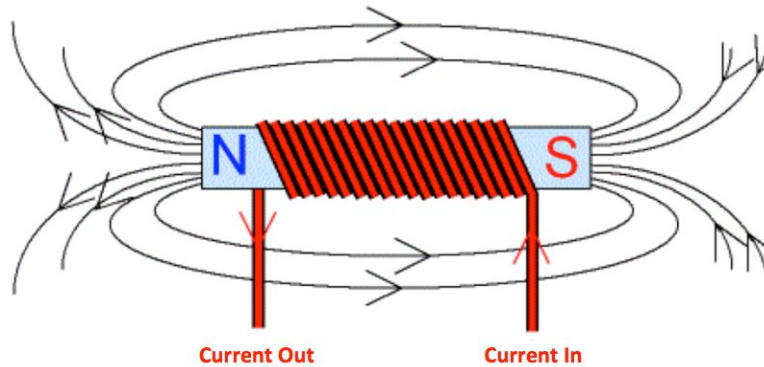


Figure 2.1: Poles of an Electromagnet

3.0 Test Facility

When searching for a suitable test facility, there were a few criteria that the team had to keep in mind. The first, the room must have an I-beam stable enough to hold a 400-pound mass. This I-beam must have at least six feet of clearance from the beam to the ground. The location of where this I-beam is located is preferred to be indoors. If this beam was located outdoors, then due to weather conditions in San Antonio in the month of October and November, our data would be introduced to another form of error. Next, the test site must also be accessible to an electrical outlet. Finally, the test site must be secluded from the public. Since the test site is located on-campus (at the University of Texas at San Antonio), students (that are not a part of team Stratos) must not be given access to the testing room.

3.1 Location

The test site is located on the ground floor of the McKinney Humanities (MH) building. The is restricted to all students and staff member, however, representatives from Graduate Studies and Research (GSR) have allowed us to set up our assembly and conduct our tests from November 1st to November 12th. Figure 3.1 and Figure 3.2 show images of the testing room.

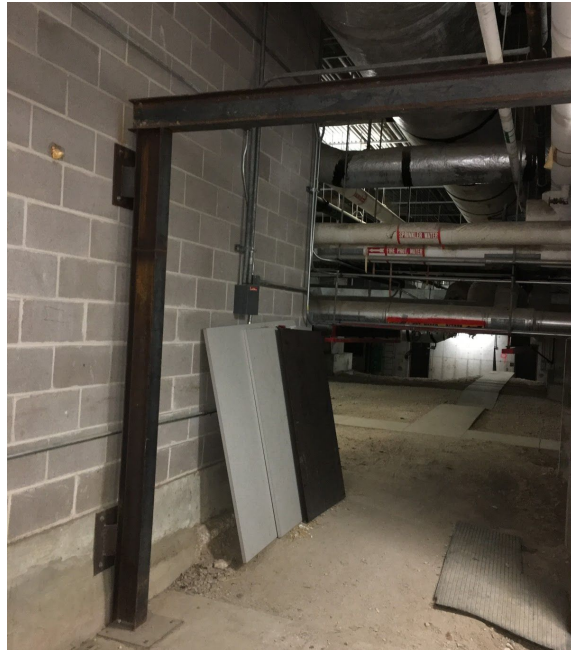


Figure 3.1: Testing Room



Figure 3.2: Testing Room

In the figures of the testing room, the team has been given a location with an I-beam to perform the experiment. Since the room is located on the ground floor of the MH building, students do not tend to visit that area. Furthermore, the room is only accessible with a key card, which is not given to students. Finally, the room is accessible to an outlet that can be used for the power supply.

3.2 Structural Integrity of the Beam

While scouting for a testing facility, GSR had helped the team search for a proper test site. When we came across the room in the MH building, the team found an I-beam that may have been suitable for our tests. The I-beam, as shown in Figures 3.1 and 3.2, is supported by three beams and welded at the top. At one end, the beam is bolted to the wall and at the other end, the beam is bolted to the ground. Therefore, when we computed the deflection of the beam, we treated it as if it is simply supported.

Before we received confirmation to use the test site, we first calculated the deflection of the beam. The material of the beam is carbon steel. The deflection of the beam, when the STAS has been placed one-third of the full length of the beam from one end, is 0.128 inches. The allowable deflection for a beam located in a gantry is 0.380, therefore, testing on this beam is claimed to be acceptable for the duration of this project. Calculations of the deflection are posted in the appendix, section A.1.

3.3 Instrumentation and Equipment

To perform the following experiment, there is some equipment that is required to record oscillation and supply power to the electromagnets. The first piece of equipment, that is necessary to record oscillation is the potentiometer. The potentiometer is located at the top of the structure, next to the pin connector. There are two gears that are attached to the bolt (that is rotating along with the structure) and the potentiometer, as shown in Figure 3.4 below.



Figure 3.3: Potentiometer

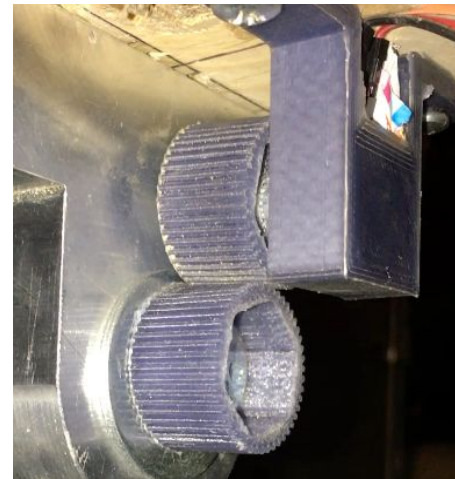


Figure 3.4: Gears to record oscillation

The next piece of equipment that is necessary for this experiment is the bearings. There are four bearings that are pressure-fitted into the pin connectors. These bearings will reduce friction as the structure is oscillating and allow the team to effectively record data.

The final two pieces of equipment have been used to supply power to the electromagnets. The first is the 14 gauge enameled copper wire that is wrapped around the cast iron core of the electromagnets. With these wires, the team can supply no more than 15 amps of current. Next, the B&K Precision power supply, that was loaned to us from our sponsor, was used to supply power to the electromagnets.



Figure 3.5: B&K Precision (Model 9115) Power Supply

3.4 Data Systems used for Testing

To record data, a potentiometer is used to record oscillation. To read the incoming voltage of the potentiometer, the team used a myDAQ from National Instruments. First, the team constructed a block diagram with the NI myDAQ and potentiometer, as shown in Figure 3.6 below. The team is then able to create a waveform chart, which allows the user to read the voltage of the potentiometer.

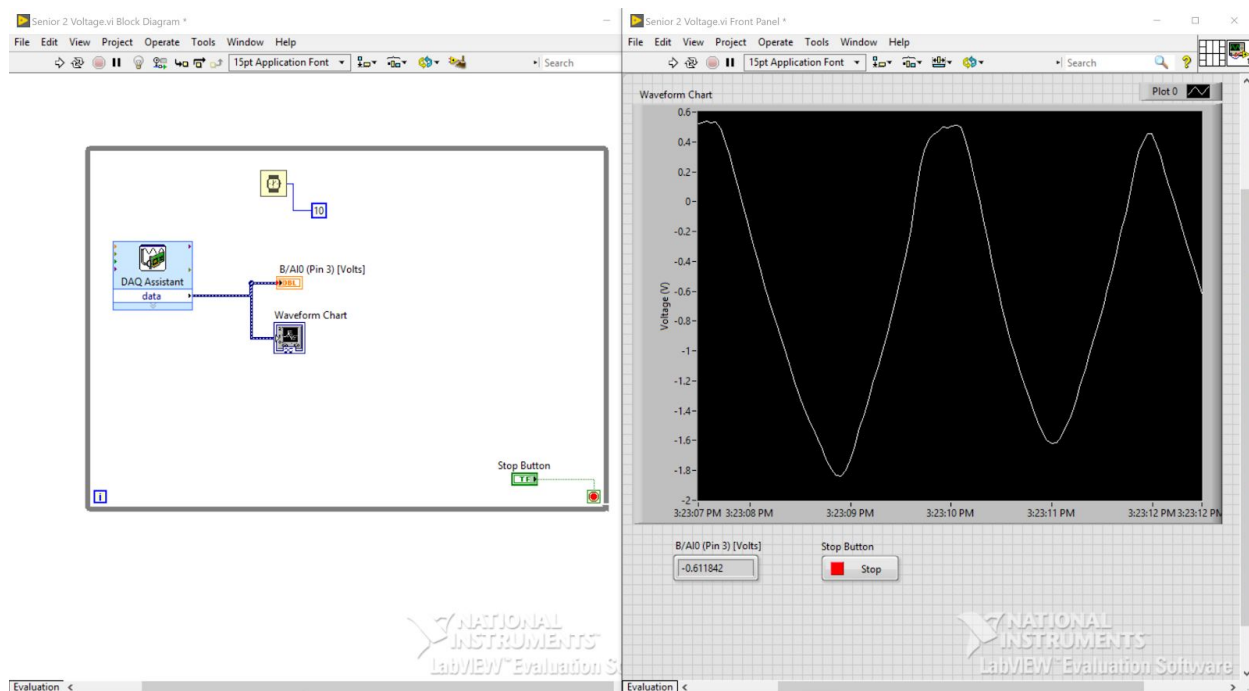


Figure 3.6: Block Diagram and Waveform Chart

4.0 Test Description

Preparation of the testing site commenced with the suspension of the STAS to the I-beam in the test site. The potentiometer was then wired and fastened to the wooden mounting bracket and connected to the NI myDAQ. The system was then inspected by the engineers before tests begin. Testing procedure consists of an engineer running the data acquisition system and signalling the team to hoist the system at the first testing angle and the first testing weight. The data acquisition engineer then signaled the team to release the system and data was recorded by the NI myDAQ. Once the NI myDAQ collected 3 minutes of data, the system was then halted, and the data exported. The same angle and weight was then tested 2 more times, before moving to the dataset. Finally, once all the datasets were collected for the undamped system, the magnetic dampers were activated and the same tests were ran for the damped system.

4.1 Test Conditions

The test site was located in the basement of the McKinney Humanities (MH) Building at the University of Texas at San Antonio. The basement is at room temperature (about 70° F), with stagnant air speed. The system test uses a simply supported steel beam at an elevation of 8 feet, that can support the system at its maximum weight of 400 lbs.

4.2 List of Instruments Required

This test required the use of the following data collection instruments: a radial potentiometer used to measure oscillation by variable resistance, a NI myDAQ system to collect and record the data measured by the potentiometer, a computer for which to view and manage the data acquisition software, and finally a power supply for the electromagnets.

4.3 Calibration Procedures and Traceability

Before testing began, the potentiometer was tested through the NI myDAQ system for adequate wiring and quality. The BNK Precision 9115 power source then needed to be calibrated to 8 volts with a current of 14 amps to activate the electromagnetic dampers. Finally, the NI myDAQ software was calibrated to ensure we collect the maximum amount of data points by recording the voltage data with respect to time.

5.0 Data Reduction and Analysis

Data gathered from the NI myDAQ is reduced to compare the peaks of each wave, which is then interpolated to create a logarithmic decrement of the oscillations. This data is then analyzed and double checked with previous recordings to ensure the data gathered is suitable.

5.1 Analysis Methods

Using the data collected by the NI myDAQ, the numbers associated with the sinusoidal graph are transcribed into excel where the difference between each peak is calculated. From this number set a logarithmic decrement can then be applied to create the graph showcasing the underdamped systems, and the change in the damping coefficient. After the data was collected into an excel spreadsheet, a t-Test was performed between the two trials performed for each test. The t-Test is one of the many types of statistics that can be performed on sets of raw data. It is used to determine whether there is a significant difference between the means of two groups. Figures 5.1 through 5.12 show the t-Test performed for all of the tests.

Undamped 100 Pounds - 15 Degrees		
t-Test: Paired Two Sample for Means		
	Variable 1	Variable 2
Mean	-0.00176	-0.00165
Variance	0.005817	0.006451
Observations	1024	1024
Pearson Correlation	0.80281	
Hypothesized Mean Difference	0	
df	1023	
t Stat	-0.06979	
P(T<=t) one-tail	0.472186	47.22%
t Critical one-tail	1.646344	
P(T<=t) two-tail	0.944371	94.44%
t Critical two-tail	1.962286	

Figure 5.1: Analysis of Undamped Trials
(15°, 100 lbs)

Damped 100 Pounds - 15 Degrees		
t-Test: Paired Two Sample for Means		
	Variable 1	Variable 2
Mean	0.000228	0.000215
Variance	0.000612	0.000497
Observations	1023	1023
Pearson Correlation	0.014414	
Hypothesized Mean Difference	0	
df	1022	
t Stat	0.012985	
P(T<=t) one-tail	0.494821	49.48%
t Critical one-tail	1.646346	
P(T<=t) two-tail	0.989643	98.96%
t Critical two-tail	1.962288	

Figure 5.2: Analysis of Damped Trials
(15°, 100 lbs)

Undamped 100 Pounds - 25 Degrees		
t-Test: Paired Two Sample for Means		
	Variable 1	Variable 2
Mean	-0.00163	-0.00159
Variance	0.006954	0.007691
Observations	1024	1024
Pearson Correlation	0.90228	
Hypothesized Mean Difference	0	
df	1023	
t Stat	-0.03383	
P(T<=t) one-tail	0.48651	48.65%
t Critical one-tail	1.646344	
P(T<=t) two-tail	0.973021	97.30%
t Critical two-tail	1.962286	

Figure 5.3: Analysis of Undamped Trials
(25°, 100 lbs)

Damped 100 Pounds - 25 Degrees		
t-Test: Paired Two Sample for Means		
	Variable 1	Variable 2
Mean	2.04497E-05	0.000257
Variance	0.00263309	0.001751
Observations	1023	1023
Pearson Correlation	0.007138419	
Hypothesized Mean Difference	0	
df	1022	
t Stat	-0.114771157	
P(T<=t) one-tail	0.454324528	45.43%
t Critical one-tail	1.646345955	
P(T<=t) two-tail	0.908649055	90.86%
t Critical two-tail	1.962287894	

Figure 5.4: Analysis of Damped Trials
(25°, 100 lbs)

Undamped 150 Pounds - 15 Degrees		
t-Test: Paired Two Sample for Means		
	Variable 1	Variable 2
Mean	-0.00181	-0.00176
Variance	0.005356	0.005008
Observations	1024	1024
Pearson Correlation	0.232457	
Hypothesized Mean Difference	0	
df	1023	
t Stat	-0.02027	
P(T<=t) one-tail	0.491917	49.19%
t Critical one-tail	1.646344	
P(T<=t) two-tail	0.983834	98.38%
t Critical two-tail	1.962286	

Figure 5.5: Analysis of Undamped Trials
(15°, 150 lbs)

Damped 150 Pounds - 15 Degrees		
t-Test: Paired Two Sample for Means		
	Variable 1	Variable 2
Mean	0.00016	0.000365
Variance	0.001255	0.001275
Observations	1023	1023
Pearson Correlation	0.020608	
Hypothesized Mean Difference	0	
df	1022	
t Stat	-0.1316	
P(T<=t) one-tail	0.447665	44.77%
t Critical one-tail	1.646346	
P(T<=t) two-tail	0.89533	89.53%
t Critical two-tail	1.962288	

Figure 5.6: Analysis of Damped Trials
(15°, 150 lbs)

Undamped 150 Pounds - 25 Degrees		
t-Test: Paired Two Sample for Means		
	Variable 1	Variable 2
Mean	-0.001983467	-0.00148
Variance	0.006469015	0.007488
Observations	1024	1024
Pearson Correlation	0.828557918	
Hypothesized Mean Difference	0	
df	1023	
t Stat	-0.327817924	
P(T<=t) one-tail	0.371558206	37.16%
t Critical one-tail	1.646344495	
P(T<=t) two-tail	0.743116411	74.3%
t Critical two-tail	1.96228562	

Figure 5.7: Analysis of Undamped Trials
(25°, 150 lbs)

Damped 150 Pounds - 25 Degrees		
t-Test: Paired Two Sample for Means		
	Variable 1	Variable 2
Mean	-0.00034	0.000191
Variance	0.002	0.001998
Observations	1023	1023
Pearson Correlation	0.011739	
Hypothesized Mean Difference	0	
df	1022	
t Stat	-0.27117	
P(T<=t) one-tail	0.393156	39.32%
t Critical one-tail	1.646346	
P(T<=t) two-tail	0.786311	78.63%
t Critical two-tail	1.962288	

Figure 5.8: Analysis of Damped Trials
(25°, 150 lbs)

Undamped 200 Pounds - 15 Degrees		
t-Test: Paired Two Sample for Means		
	Variable 1	Variable 2
Mean	-0.00183376	-0.00203
Variance	0.007270324	0.006603
Observations	1024	1024
Pearson Correlation	0.956590287	
Hypothesized Mean Difference	0	
df	1023	
t Stat	0.251544059	
P(T<=t) one-tail	0.400722012	40.07%
t Critical one-tail	1.646344495	
P(T<=t) two-tail	0.801444023	80.14%
t Critical two-tail	1.96228562	

Figure 5.9: Analysis of Undamped Trials
(15°, 200 lbs)

Damped 200 Pounds - 15 Degrees		
t-Test: Paired Two Sample for Means		
	Variable 1	Variable 2
Mean	9.33E-05	0.000107
Variance	0.002094	0.001761
Observations	1023	1023
Pearson Correlation	-0.02964	
Hypothesized Mean Difference	0	
df	1022	
t Stat	-0.00714	
P(T<=t) one-tail	0.497152	49.72%
t Critical one-tail	1.646346	
P(T<=t) two-tail	0.994303	99.43%
t Critical two-tail	1.962288	

Figure 5.10: Analysis of Damped Trials
(15°, 200 lbs)

Undamped 200 Pounds - 25 Degrees		
t-Test: Paired Two Sample for Means		
	Variable 1	Variable 2
Mean	-0.00191	-0.00165
Variance	0.007145	0.007869
Observations	1024	1024
Pearson Correlation	0.123249	
Hypothesized Mean Difference	0	
df	1023	
t Stat	-0.07184	
P(T<=t) one-tail	0.471371	47.14%
t Critical one-tail	1.646344	
P(T<=t) two-tail	0.942742	94.27%
t Critical two-tail	1.962286	

Figure 5.11: Analysis of Undamped Trials
(25°, 200 lbs)

Damped 200 Pounds - 25 Degrees		
t-Test: Paired Two Sample for Means		
	Variable 1	Variable 2
Mean	-0.00052	0.000207
Variance	0.004217	0.004464
Observations	1023	1023
Pearson Correlation	-0.00314	
Hypothesized Mean Difference	0	
df	1022	
t Stat	-0.2498	
P(T<=t) one-tail	0.401396	40.14%
t Critical one-tail	1.646346	
P(T<=t) two-tail	0.802792	80.28%
t Critical two-tail	1.962288	

Figure 5.12: Analysis of Damped Trials
(25°, 200 lbs)

5.2 Verification of Test Results

Data will be proofread to check for consistencies in creating a depreciating sinusoidal wave pattern. Multiple trials are also conducted to ensure repeatability of results. With both of these methods of verification it is shown that the data gathered is reliable, and represents the physical occurrences that it is representing. From our multiple trials conducted the statistical analysis is statistically significant with the exception of a few: Figures 5.7, 5.8, 5.9, and 5.12. These certain t-Tests showed a significant difference with a probability less than eighty five percent.

5.3 Error Analysis

There was some error in the data that was collected. One source of error occurred when the beam twisted during testing, causing the NI myDAQ to give false readings. During the data collection there were several wire checks, which the team ended up switching to an extended USB cable due to errors encountered. Also, while using an extended USB wire, if there was any interference or disturbance of the wire, this would cause false readings as well. Potentiometers were also tested before the data collection, and switched out during the data collection to ensure that they were reading correctly. In Figure 5.13, the graph depicts the error that was encountered by the twisting I-beam, the wiring used to connect the NI myDAQ, and the potentiometer. Also, without the use of a low passive filter connected to our system this would account for error in our analysis as well. The errors encountered during testing were determined to be most likely caused by instrumentation error, not human error.

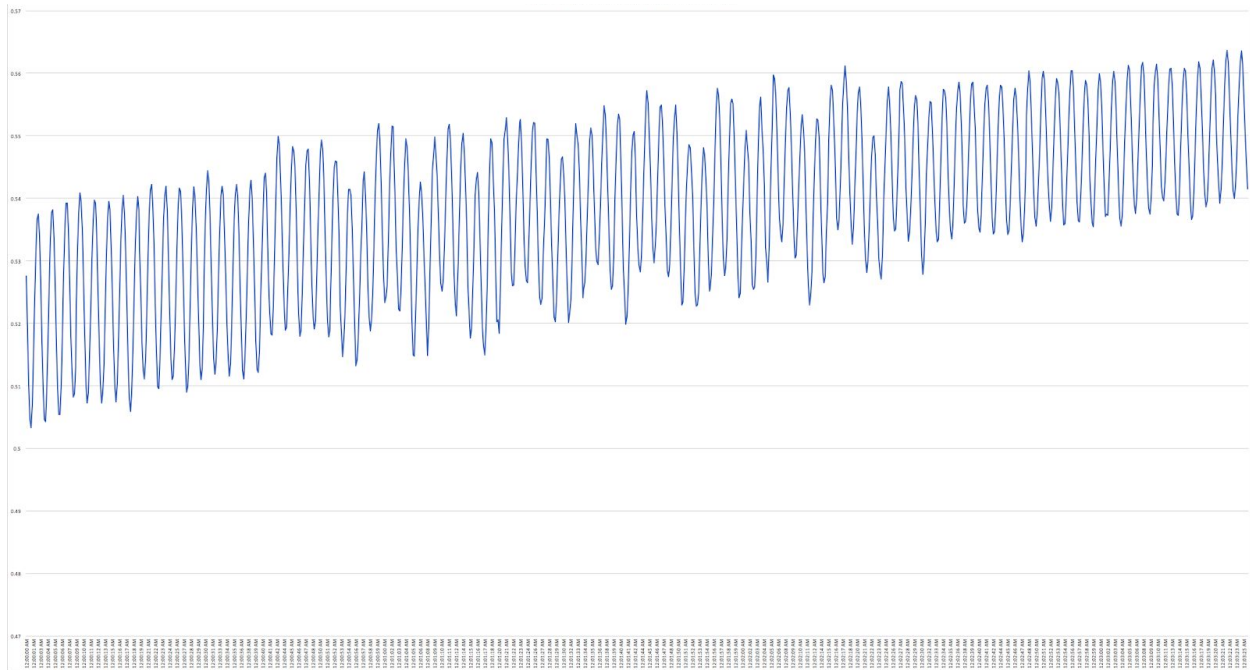


Figure 5.13: Oscillation Graph with a 200 lb passenger mass at 15 degrees

6.0 Reported Results

In this experiment, the team graphed the oscillation for three passenger masses at two different angles of attack. For each test performed, there were at least three trials conducted. Therefore, the total number of tests performed was 36.

Figures 6.1 and 6.2 show the oscillation graph of the system with a 100 pound passenger mass at an angle of attack of 15 degrees from the vertical axis.

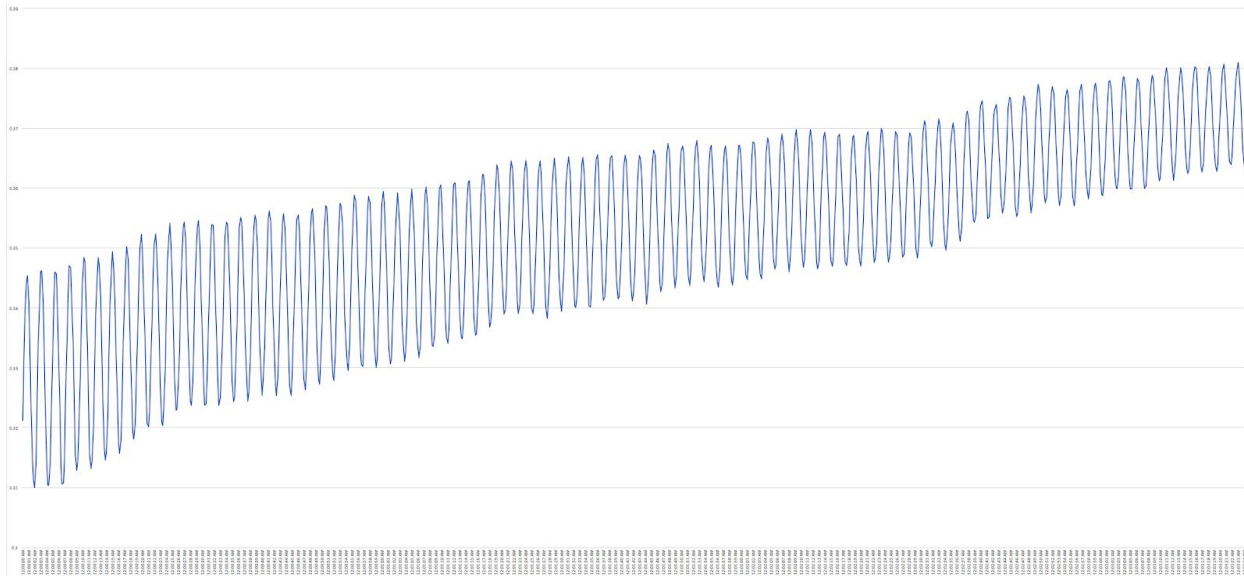


Figure 6.1: Damped Oscillation (with a 100 lb passenger mass at 15 degrees)

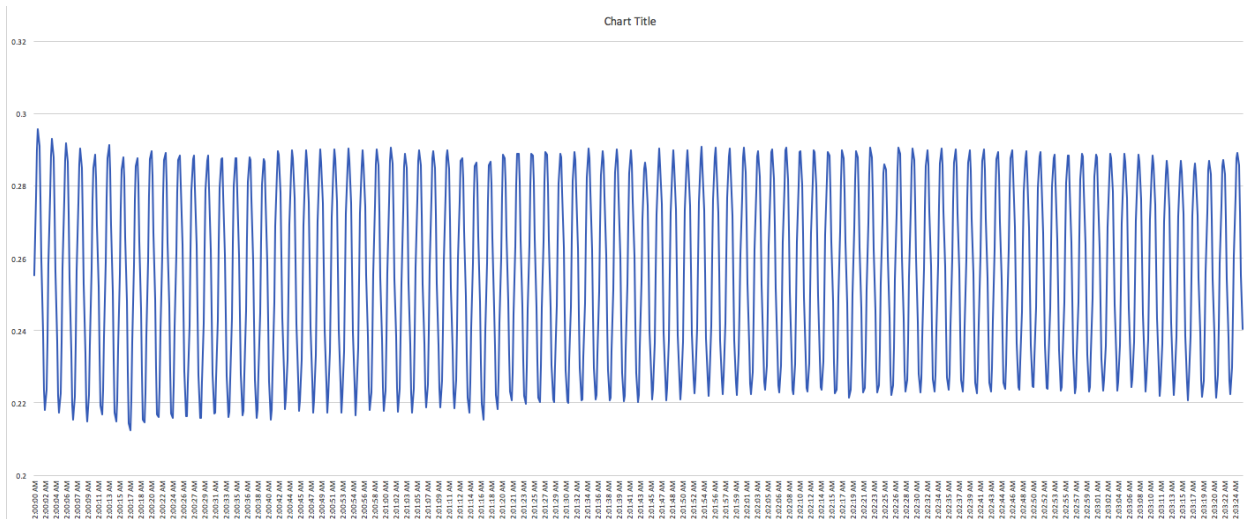


Figure 6.2: Undamped Oscillation (with a 100 lb passenger mass at 15 degrees)

6.1 Populated Table

Table 6.1: Populated Test Table

Test Number	Angle from vertical axis	Passenger Mass (lb)	T (s)	ζ (%)
1	15° Undamped	100	3	0.0959662
2		150	2	0.0463177
3		200	3	0.0147945
4	25° Undamped	100	2	0.09926
5		150	2	0.03089
6		200	3	0.02988
7	15° Damped	100	2	9.06893356
8		150	3	6.05591183
9		200	2	5.36963555
10	25° Damped	100	3	8.36455913
11		150	3	6.93629412
12		200	3	5.61889047

6.2 Results Support of Conclusion

As shown by the populated table and Figures 6.1 and 6.2 (which displays the undamped and damped graph, respectively), the effective damping with the use of electromagnetic dampers is greater than the effective damping without it. Table 6.1 displays the effective damping of the system with and without the use of the electromagnetic dampers. From the table, the effective damping with a passenger mass of 100 pounds (regardless of whether or not the electromagnets are in use) is greater than the effective damping with a 150 and 200 pound passenger mass. As predicted, the electromagnetic dampers have been able to effectively increase damping.

7.0 Schedule

Figure 7.1 below displays the Gantt Chart which shows the all of the major assignments completed by the team in the Senior Design 2 semester. Table 7.1 shows a detailed layout of the Gantt Chart which lists all of the major tasks completed with the date at which this task began and ended.

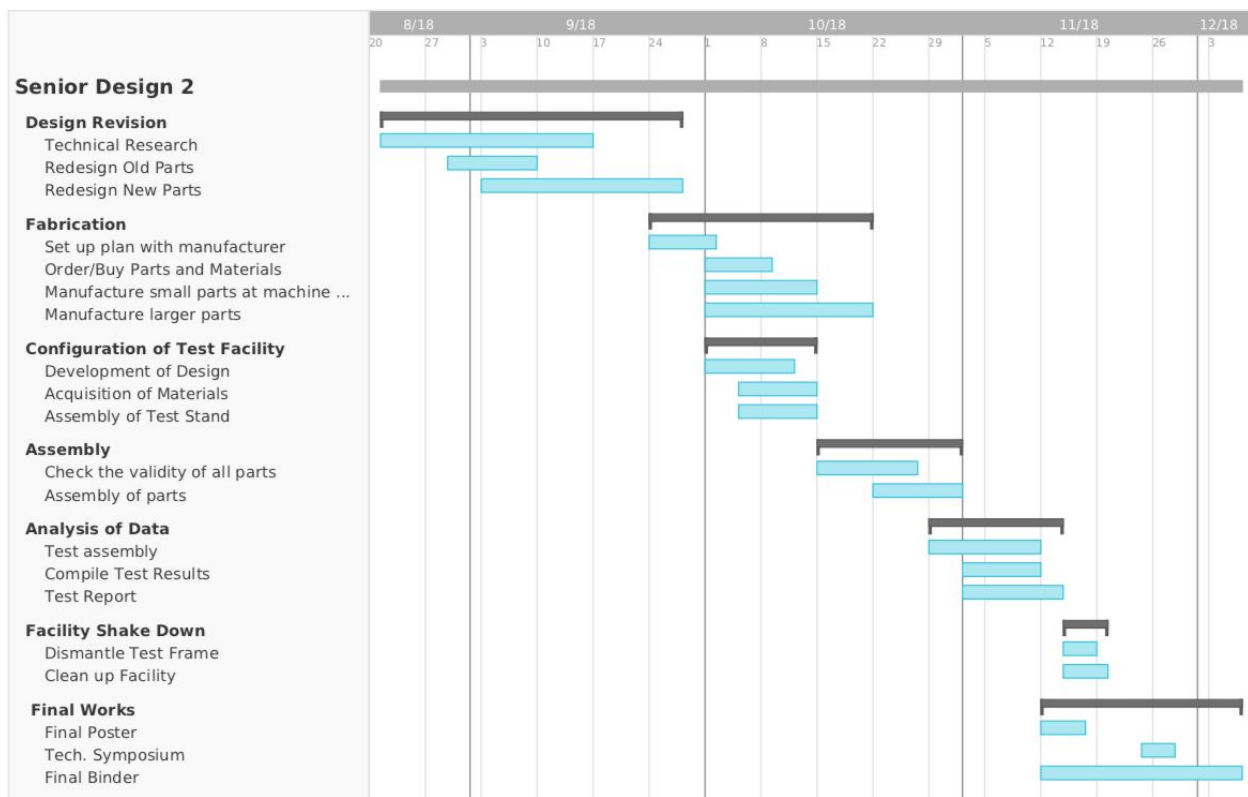


Figure 7.1: Gantt Chart

Task		Start Date	End Date	Percent Completion
Design Revisions	Technical Research	Aug-21	Sep 14	100%
	Redesign Old Parts	Aug-29	Sep 7	100%
	Redesign New Parts	Sep-3	Sep 26	100%
Fabrication	Set up plan with manufacturer	Sep 24	Oct 1	100%
	Order Parts and Materials	Oct 1	Oct 12	100%
	Fabrication at ITM	Oct 1	Oct 19	100%
	Fabrication at UTSA machine shop	Oct 8	Nov 5	100%
Assembly	Check parts with their drawing	Oct 24	Nov 2	100%
	Assembly of Parts	Oct 31	Nov 6	100%
Configuration of Test Facility	Development of Design	Oct 25	Oct 26	100%
	Acquisition of Materials	Oct 29	Oct 31	100%
Testing and Analysis of Data	Test Assembly	Nov 1	Nov 9	100%
	Testing	Nov 7	Nov 12	100%
	Compile Test Results	Nov 7	Nov 12	100%
	Test Report	Nov 8	Nov 13	100%
Facility Shakedown	Dismantle Test Assembly	Nov 14	Nov 16	100%
	Clean up Facility	Nov 16	Nov 16	100%
Final Work	Final Poster	Nov 12	Nov 15	100%
	Tech. Symposium	Nov 27	Nov 27	100%
	Final Report	Nov 14	Dec 5	100%
	Final Binder	Nov 12	Dec 5	100%

Table 7.1: Percent Complete by Task

8.0 Conclusions and Recommendations

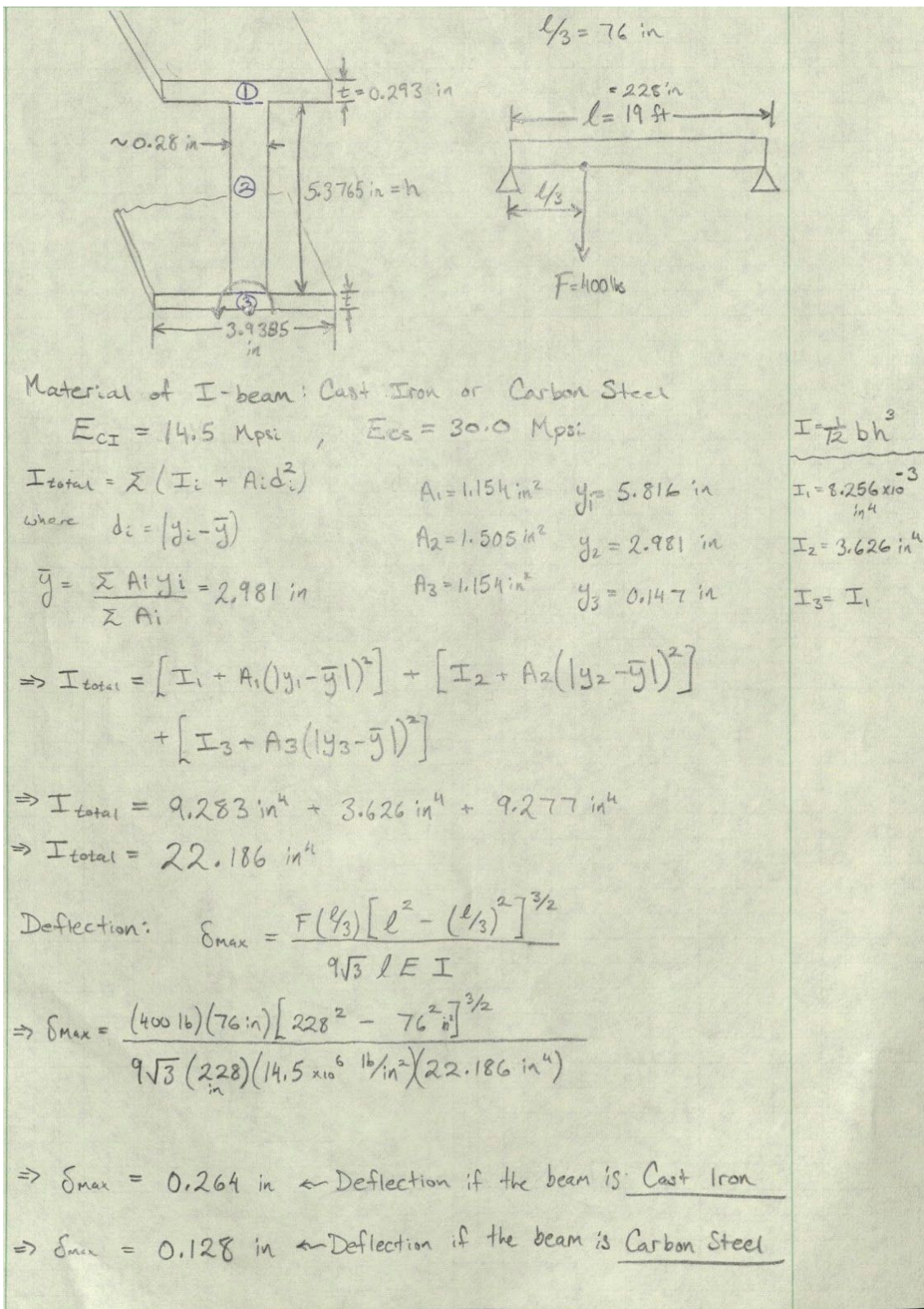
The data gathered here demonstrates an increase in the damping coefficient of the system. However from the data collected it is shown that a major increase in the current supplied, and power of magnets is needed to reach the goal of an effective method of damping the oscillating system. For both systems the time it took to settle was greater than three minutes, which means the drone would have to sit for three minutes or more in order to have a stable payload. Still, the electromagnetic dampers did have an affect on the system, reducing the settling time compared to the undamped system which was allowed to oscillate freely and had a far greater settling time. The electromagnets were acting as intended, with each set having the corresponding polarity, and was determined to have a strong magnetic force. A complete redesign of the shafts experiencing the magnetic forces would be necessary to increase the effective damping. However due to the power consumption required, finding the means for a passive or non electrical reactive damper is recommended. Design of a variable aerodynamic damper that increases in drag during oscillation, but must also have minimum drag while travelling could solve these problems. This method of design could allow for a purely mechanical support that does not require its own power supply.

9.0 Communication

Communications on all aspects of the test program on a regular basis is encouraged. The primary technical contact at the University of Texas at San Antonio is any of the members of Team Stratos; Daniel Jiwani (210-836-4316), Cristian Morales (210-831-9239), Chad Parker (210-355-4760) or William Hinojosa (512-569-1145). Questions of a contractual nature should be addressed to Dr. Pranav Bhounsule (pranav.bhounsule@utsa.edu)

Appendix

A.1 Beam Deflection Calculations



A.2 Design Specifications

Please refer to Appendix E of this Final Binder for the Design Specification of the Sky Transportation Attachment System.